

学位論文（要約）

**Studies on diversification of organelles and
membrane trafficking pathways using *Marchantia polymorpha***
(ゼニゴケを用いたオルガネラと膜交通経路の多様化の研究)

平成 28 年 12 月博士（理学）申請

東京大学大学院理学系研究科

生物科学専攻

金澤建彦

**Studies on diversification of organelles and
membrane trafficking pathways using *Marchantia polymorpha***

Takehiko Kanazawa

2016

Department of Biological Sciences

Graduate School of Science

The University of Tokyo

Abstract

Membrane traffic is a fundamental system responsible for correct transport and localization of proteins, lipids, and polysaccharides in eukaryotic organisms including plants. Among key machinery components of membrane trafficking, Rab GTPases and SNARE proteins mediate tethering and fusion between transport vesicles and target membranes, respectively. Although the molecular framework is well conserved in eukaryotic lineages, it is also known that each eukaryotic lineage has acquired lineage-specific membrane trafficking pathways during evolution, which should be involved in lineage-specific biological functions. The diversification of membrane trafficking is considered to result from, at least partly, functional differentiation of the machinery components such as Rab GTPases and SNARE proteins. However, its detailed mechanisms remain almost unknown. In this study, I aimed to unveil how membrane trafficking pathways have diversified during land plant evolution using the liverwort, *Marchantia polymorpha*, which is an emerging model of basal land plants, with a special interest in SNARE molecules.

I identified 34 genes for SNARE proteins in *M. polymorpha* based on the genome and transcriptome information. I then examined subcellular localization of the majority of these SNARE molecules by expressing fluorescently tagged proteins in *M. polymorpha* thallus tissues. The results obtained and comparison with the subcellular localization of orthologous products in *Arabidopsis thaliana* indicated that the membrane trafficking system has increased its complexity during land plant evolution. Through this analysis, I also succeeded in establishing reliable endomembranous organelle markers in *M. polymorpha* (Chapter III).

I then carried out detailed analyses for the SYP1 group, which is remarkably

expanded in seed plants, in *M. polymorpha*. I found that one of four SYP1 members in *M. polymorpha* plays an essential role in cell plate formation during cytokinesis, while its close relative is specifically expressed in oil body cells and localized to the membrane of the oil body, an organelle unique to liverworts. Observation of various organelle marker proteins and a secretory cargo in dividing cells and in oil body cells indicated that targeting to these organelles is accomplished by transient redirection of the secretory pathway. Furthermore, I found that none of the known organelle markers are localized to the oil body membrane, although previous studies proposed several possible organelles as origins of this liverwort-specific compartment. These results indicated that functional diversification of SYP1 members accompanied with transient alteration of transport destinations should contribute to the acquisition of new organelles in the plant lineage (Chapter IV).

For insights into molecular mechanisms of biogenesis of the oil body in *M. polymorpha*, I then conducted forward genetic screening for mutant plants with altered oil body morphology or distribution patterns. I have successfully isolated several putative mutants from 16,000 T-DNA-tagged lines, which will be useful to unravel how and why liverworts attained the oil body during evolution (Chapter V).

Contents

Abstract	1
Acknowledgements	4
Abbreviations	5
Chapter I: General Introduction	7
Chapter II: Materials and Methods	12
Figure and Tables	20
Chapter III: Characterization of SNARE molecules of <i>Marchantia polymorpha</i>	
Introduction	26
Results	28
Discussion	38
Figures	46
Chapter IV: Cell-specific redirection of the secretory trafficking pathway lead to acquisition of new organelles during land plant evolution	
Introduction	65
Results	71
Discussion	79
Figures	88
Chapter V: Screening for mutants of oil body biogenesis and morphogenesis	
Introduction	107
Results	108
Discussion	112
Figures and Table	115
Chapter VI: Conclusion	121
References	124

Acknowledgements

First of all, I would like to express my deepest gratitude to my supervisors, Dr. Takashi Ueda and Dr. Akihiko Nakano for giving me opportunity to study in their laboratories and for supervision and encouragement throughout this study. I would like to thank Dr. Hirokazu Tsukaya, Dr. Hiroyuki Takeda and Dr. Hisayoshi Nozaki for critical comments on this thesis. I would also like to thank Dr. Takayuki Kohchi (Kyoto University), Dr. Katsuyuki T. Yamato (Kindai University), Dr. Kiyohiko Igarashi (The University of Tokyo), Dr. Kimitsune Ishizaki (Kobe University), Dr. Ryuichi Nishihama (Kyoto University), Dr. Masaru Fujimoto (The University of Tokyo), Dr. Takumi Higaki (The University of Tokyo), Dr. Shohei Yamaoka (Kyoto University), Dr. Tomoaki Nishiyama (Kanazawa University), Dr. Shigeo S. Sugano (Tokushima University) and Ms. Sakiko Ishida (Kyoto University) for kindly sharing materials and unpublished information and for supporting this research. I am also grateful to Dr. Tomohiro Uemura, Dr. Kazuo Ebine, Dr. Tomokazu Tsutsui, Dr. Takashi L. Shimada, Dr. Atsuko Era, Mr. Naoki Minamino, Mr. Yu Shikano, Ms. Hatsune Morinaka, Mr. Takuya Norizuki, Ms. Hiromi Takahashi, Ms. Yuko Shiihara, and Ms. Masayo Ookubo for technical supports, valuable discussion, and kind encouragement.

I also thank the Data Integration and Analysis Facility and Spectrography and Bioimaging Facility of National Institute for Basic Biology for computational resources for support in phylogenetic analyses and technical supports.

Abbreviations

AP2/ERF: APETALA2/ethylene-responsive element binding factors

BF: bright field

BODIPY 493/503: 4,4-difluoro-1,3,5,7,8-pentamethyl-4-bora-3a,4a-diaza-*s*-indacene

BSA: bovine serum albumin

CaMV: cauliflower mosaic virus

CCV: clathrin-coated vesicle

CRISPR/Cas9: clustered regularly interspaced short palindromic repeats-associated endonuclease Cas9 system

ER: endoplasmic reticulum

EYFP: enhanced yellow fluorescent protein

FM4-64: *N*-(3-triethylammoniumpropyl)-4-(6-(4-(diethylamino)phenyl)hexatrienyl)pyridinium dibromide

GA: glutaraldehyde

GEF: guanine nucleotide exchange factor

gRNA: guide RNA

mCitrine: monomeric Citrine

mGFP: monomeric green fluorescent protein

mRFP: monomeric red fluorescent protein

MSA: mitosis-specific activator

Myr-VAMP72: *N*-myristoylated VAMP72

ORF: open reading frame

PBS: phosphate buffered saline

PCR: polymerase chain reaction

PFA: paraformaldehyde

PM: plasma membrane

PVC: prevacuolar compartment

RT-PCR: reverse transcription PCR

SNARE: soluble *N*-ethylmaleimide-sensitive factor attachment protein receptor

SP: signal peptide

ST: sialyltransferase

TAIL-PCR: thermal asymmetric interlaced-PCR

T-DNA: transfer DNA

TEM: transmission electron microscope

TGN: *trans*-Golgi network

TMD: transmembrane domain

YFP: yellow fluorescent protein

Chapter I: **General Introduction**

Membrane traffic is a fundamental system responsible for precise transport and localization of proteins, lipids, and polysaccharides among single membrane-bounded organelles, the plasma membrane (PM), and the extracellular space, which is essential for homeostasis and precise functions of cells and organelles. The basic molecular framework underlying membrane trafficking is evolutionarily conserved among eukaryotes, which comprises four sequential processes: 1) sorting cargoes and forming transport vesicles on donor organelle membranes, 2) conveying transport vesicles, 3) tethering transport vesicles to target organelle membranes, and 4) fusing transport vesicles with target organelle membranes. Each of these processes is strictly controlled by evolutionarily conserved machinery components, which include coat protein complexes and Rab GTPases responsible for formation of transport vesicles at donor membranes and tethering of the transport vesicles to target organelle membranes, respectively (Fujimoto & Ueda, 2012). Soluble *N*-ethylmaleimide-sensitive factor attachment protein receptor (SNARE) is another evolutionarily-conserved component that functions at the final process of membrane trafficking, executing membrane fusion of organelles or transport vesicles with destination membranes (Sollner *et al.*, 1993a; Sollner *et al.*, 1993b). SNARE molecules are distinguished by the highly conserved helical region, referred to as the SNARE motif. SNARE molecules are divided into two classes, Q- and R-SNAREs according to the amino acid residue (Q, glutamine or R, arginine) at the distinctive position of the SNARE motif, referred to as the zero layer. In many cases, R-SNAREs are localized to transport vesicles and Q-SNAREs reside on target organelle membranes. Q-

SNAREs are further classified into Qa-, Qb-, Qc-, and Qb+Qc-SNAREs based on the similarity and the number of the SNARE motif (Fasshauer *et al.*, 1998; Bock *et al.*, 2001; Antonin *et al.*, 2002). Specific combinations of four SNARE motifs, each of which is supplied by Qa-, Qb-, Qc-, and R-SNARE proteins or by Qa-, Qb+Qc-, and R-SNARE proteins, assemble into a tight complex, which results in membrane fusion of transport vesicles with target organelles. The repertoire of SNARE proteins and their functions are well conserved among eukaryotic lineages, including animals, yeasts, and plants (Hong, 2005; Dacks & Field, 2007; Sanderfoot, 2007).

In addition to fundamental roles at the cellular level, membrane trafficking fulfills various higher-ordered functions in animals and plants. In land plants, various higher-ordered and plant-unique processes are reported to depend on the membrane trafficking system, including cell wall synthesis/remodeling, polar transport of auxin, embryogenesis, abiotic/biotic stress responses, and gravitropism (Lukowitz *et al.*, 1996; Geldner *et al.*, 2001; Kato *et al.*, 2002; Morita *et al.*, 2002; Collins *et al.*, 2003; Yano *et al.*, 2003; Leshem *et al.*, 2006; Petrasek *et al.*, 2006; Wisniewska *et al.*, 2006; Crowell *et al.*, 2009; Gutierrez *et al.*, 2009; Asaoka *et al.*, 2012; Uemura *et al.*, 2012; Hashiguchi *et al.*, 2014; Inada & Ueda, 2014; Kim & Brandizzi, 2014; Tanaka *et al.*, 2014; Uehara *et al.*, 2014). These diverse and specialized functions appear to result from land plants pioneer novel trafficking pathways accompanied by acquisition of new and land-plant-specific machinery components for membrane trafficking (Fujimoto & Ueda, 2012). For instance, VAMP727, an R-SNARE protein unique to seed plants with a typical insertion in its longin domain, plays significant roles in development and germination of the seeds in *Arabidopsis thaliana* (Ebine *et al.*, 2008). A member of RAB5 GTPases, ARA6, which is highly conserved in land plants and functions in endosomal trafficking, is also a notable

example uniquely acquired during plant evolution (Ueda *et al.*, 2001; Ebine *et al.*, 2011). Evolutionarily conserved machineries such as RAB5 and RAB7 are also shown to be recruited to different trafficking pathways between animals and land plants (Cui *et al.*, 2014; Ebine *et al.*, 2014; Singh *et al.*, 2014). Thus plants, especially seed plants, have acquired specific and novel membrane trafficking pathways.

It has been proposed that the diversification of components involved in membrane trafficking was achieved by reiterating multiplication of corresponding genes followed by accumulation of mutations leading to functional differentiation (Dacks & Field, 2007). In the green plant lineage, the remarkable expansion of genes involved in membrane trafficking has been considered to accompany terrestrialization and/or multicellularization of plants (Sanderfoot *et al.*, 2000; Rutherford & Moore, 2002; Dacks & Field, 2007; Sanderfoot, 2007). The diversification of SNARE molecules involved in the secretory pathway is especially apparent. The Qa-SNARE SYP1 group, which is composed of three subgroups (SYP11, SYP12, and SYP13) in seed plants and predominantly localized to the PM, is one of the most diversified SNARE molecules in land plants. SYP111/KNOLLE is specifically expressed in dividing cells and plays an essential role in formation of the cell plate to accomplish cytokinesis in *A. thaliana* (Lukowitz *et al.*, 1996; Lauber *et al.*, 1997). SYP121/PEN1/SYR1 is responsible for non-host penetration resistance against barley powdery mildew fungus in *A. thaliana* (Collins *et al.*, 2003; Kwon *et al.*, 2008). SYP121 is also reported to mediate the regulation of PM-resident ion channels (Sutter *et al.*, 2006; Honsbein *et al.*, 2009; Grefen *et al.*, 2010; Grefen *et al.*, 2015). For the SYP13 subgroup, SYP132 is ubiquitously expressed and is considered to execute constitutive secretion in *A. thaliana* plants, and also functions in tip-growing root hair cells in collaboration with SYP123, whereas its paralog SYP131 is

limitedly expressed in pollen grains (Enami *et al.*, 2009; Ichikawa *et al.*, 2014).

The relevance between the diversification of machinery components of membrane trafficking and terrestrialization and/or multicellularization in the green plant lineage has been mainly proposed by comparative genomics; the number of SNARE proteins encoded in the genome of the moss, *Physcomitrella patens*, is larger compared with unicellular green algal species (Sanderfoot, 2007). However, the knowledge regarding the organization, subcellular localization, and neofunctionalization of SNAREs in these species remains limited. *P. patens* has been shown to undergo large-scale genome duplications during evolution (Rensing *et al.*, 2007; Rensing *et al.*, 2008), which might imply that the increase of the number of SNARE genes in *P. patens* indicates the existence of paralogous genes without remarkable neofunctionalization. To gather more knowledge on the diversification of membrane trafficking in the evolutionary process of the green plant lineage, information from other basal land-plant lineages such as bryophytes (liverworts, mosses, and hornworts) and charophyte algae is apparently needed.

Marchantia polymorpha is a member of Marchantiophyta (liverwort), which are considered to occupy a basal position in phylogeny of terrestrial plants, while which lineage of the bryophytes is basalmost remains debatable (Qiu *et al.*, 2006; Wickett *et al.*, 2014). In this study, *M. polymorpha* has been selected as a model of liverworts because genome and transcriptome information is available, and genetical and cell biological techniques, including agrobacterium-mediated transformation, gene targeting, and genome editing, have been established (Chiyoda *et al.*, 2007; Ishizaki *et al.*, 2008; Era *et al.*, 2009; Era *et al.*, 2013; Ishizaki *et al.*, 2013; Kubota *et al.*, 2013; Tsuboyama & Kodama, 2013; Sugano *et al.*, 2014; Ishizaki *et al.*, 2015; Kanazawa, 2015; Tsuboyama-Tanaka & Kodama, 2015). In order to acquire the knowledge on diversification of

organelle functions and membrane trafficking pathways, I systematically analyzed organization, subcellular localization, and functions of SNARE molecules in this emerging model plant, which provided key insights into diversification of membrane trafficking during land plant evolution.

Chapter II: **Materials and Methods**

Identification of genes of *M. polymorpha* and phylogenetic analyses

Similarity search for *M. polymorpha* genes was executed using proteins of *A. thaliana* as queries as previously described in Kato *et al.* (2015) with version 3.1. Phylogenetic analysis in Figure 3-2 was performed as previously described (Banks *et al.*, 2011), with updated datasets. The dataset was as of Jan 17, 2015. Additional datasets of *Klebsormidium flaccidum* (Hori *et al.*, 2014, http://www.plantmorphogenesis.bio.titech.ac.jp/~algae_genome_project/klebsormidium/kf_download/131203_kfl_initial_genesets_v1.0_AA.fasta), *Physcomitrella patens* v1.6 (Zimmer *et al.*, 2013, https://www.cosmoss.org/physcome_project/linked_stuff/Annotation/V1.6/P.patens.V6_filtered_cosmoss_proteins.fas.gz), and *Pinus taeda* (Neale *et al.*, 2014, http://loblolly.ucdavis.edu/bipod/ftp/Genome_Data/genome/pinerefseq/Pita/v1.01/Pita_Annotation_v2/) were included. After retrieving 1000 similar sequences, the *M. polymorpha* SNARE sequences were merged and 1000 similar sequences were selected again, aligned with MAFFT v6.811b (Katoh & Toh, 2008), and a conserved sequence region was manually selected with MacClade 4 (Maddison & Maddison, 2000). The Neighbor Joining (Saitou & Nei, 1987) tree using maximum likelihood distance under the JTT model (Jones *et al.*, 1992) was constructed by using PHYLIP package 3.695 (Felsenstein, 2013). Bootstrap analysis was performed by resampling 1000 sets. After reviewing the large tree, sequences were further selected to retain the diversity but fit into a page and the phylogenetic analysis was repeated.

For Figure 5-3, sequences with AP2 domain were collected from *M. polymorpha*

genome database version 3.1 and *A. thaliana* genome database TAIR annotation version 10. Sequences were aligned with MUSCLE program version 3.8.31 (Edgar, 2004), and a conserved sequence region was manually selected, and the phylogenetic tree was constructed by PhyML program version 3.0 (Guindon *et al.*, 2010) under the LG model (Le *et al.*, 2008). Bootstrap analysis was performed by resampling 1000 sets.

Plant materials and transformation

The *M. polymorpha* male and female accessions Takaragaike-1 (Tak-1) and Takaragaike-2 (Tak-2), respectively (Ishizaki *et al.*, 2008), were used in this study. The gemmae and thalli were grown asexually on 1/2× Gamborg's B5 medium (Gamborg *et al.*, 1968) with 1.4% (w/v) agar at 22°C under continuous white fluorescent light. F1 spores were generated by crossing Tak-1 and Tak-2. The transition from the vegetative phase to the reproductive phase was induced by far-red illumination as previously described (Chiyoda *et al.*, 2008). Transformation of *M. polymorpha* was carried out according to previously described methods using the sporelings or excised thalli mediated by *Agrobacterium tumefaciens* strain GV2260 (Ishizaki *et al.*, 2008; Kubota *et al.*, 2013). Transgenic liverworts were selected on plates containing 10 mg/L hygromycin B and 100 mg/L cefotaxime or 0.5 µM chlorsulfuron and 100 mg/L cefotaxime (Ishizaki *et al.*, 2015).

Reverse transcription polymerase chain reaction (RT-PCR)

Total RNA from 5-day-old thalli, antheridiophores, archegoniophores, and 7-day-old sporelings was isolated by the RNeasy Plant Mini Kit (Qiagen) and was used as templates for reverse transcription using SuperScript III Reverse Transcriptase (Invitrogen) and the oligo dT (18 mer) primer according to the manufacturer's instructions.

The cDNA was used for polymerase chain reaction (PCR) analyses. The primer sequences were listed in Table 2-1. The expression of Mp*EF1 α* was used as a positive control.

Constructs

Open reading frames (ORFs) and genomic sequences of *M. polymorpha* genes were respectively amplified by PCR from cDNA and genome DNA prepared from the *M. polymorpha* accession Tak-1, and the PCR products were subcloned into pENTRTM/D-TOPO (Invitrogen) according to the manufacturer's instructions. The oligonucleotide sequences used in PCR are listed in Table 2-1. To construct *mCitrine-MpSYP12A*, *mCitrine-MpSYP12B*, *mCitrine-MpSYP13A*, *mCitrine-MpSYP13B*, and *mCitrine-MpSYP2*, genomic sequences comprising the 5' flanking sequences (promoter + 5' UTR), protein-coding regions, introns, and 3' flanking sequences (7.0 kb for Mp*SYP12A*, 7.4 kb for Mp*SYP12B*, 9.8 kb for Mp*SYP13A*, 7.1 kb for Mp*SYP13B*, and 8.8 kb for Mp*SYP2*) were amplified and subcloned into the pENTR vectors. Next, the cDNA for mCitrine was inserted into the 5' end of the protein-coding region using the In-Fusion HD Cloning System (Clontech) according to the manufacturer's instructions. To construct pMpGWB301-derived gateway vectors (*proMpSYP12A:mCitrine-GW*, *proMpCYCB1:mCitrine-GW* and *proMpSYP12B:mCitrine-GW*), the promoter:*mCitrine* sequences were amplified from genomic construct described above, and was inserted into the *Hind*III site of pMpGWB301 using the In-Fusion HD Cloning System. For the transformation of *M. polymorpha*, the resultant entry sequences were introduced into pMpGWB series (Ishizaki *et al.*, 2015) and modified pMpGWB (described above) for with Gateway LR ClonaseTM II Enzyme Mix (Invitrogen) according to the manufacturer's instructions. For genome editing mediated by the clustered regularly interspaced short

palindromic repeats-associated endonuclease Cas9 system (CRISPR/Cas9), target sequences were inserted into the *BsaI* site of the pMpGE_En03 entry vector (Sugano *et al.*, unpublished). The resultant sequences were then introduced into pMpGE010 or pMpGE011 (Sugano *et al.*, unpublished) using the Gateway LR Clonase™ II Enzyme Mix. For transient expression in protoplasts of *A. thaliana*, subcloned cDNA or mutated sequences with fluorescent proteins were transferred into the p2GWY vector (Karimi *et al.*, 2005).

Transient expression in protoplasts of *A. thaliana* suspension cultured cells

Transient expression of chimeric proteins of the N-terminal sequences of VAMP72 members with enhanced yellow fluorescent protein (EYFP) in *A. thaliana* cells cultured in suspension was performed as previously described (Ueda *et al.*, 2001; Uemura *et al.*, 2004). Protoplasts of *A. thaliana* were prepared by incubation of approximately 2 g of the cultured cells in 25 mL enzyme solution (400 mM mannitol, 5 mM EGTA, 1% (w/v) cellulase Y-C, and 0.05% (w/v) Pectolyase Y-23). Protoplasts were washed twice by wash buffer (400 mM mannitol, 70 mM CaCl₂, and 5 mM MES-KOH (pH 5.7)) and resuspended in MaMg solution (400 mM mannitol, 15 mM MgCl₂, and 5 mM MES-KOH, pH 5.7). The suspended protoplasts, plasmid, and single-strand carrier DNA were mixed with DNA uptake solution (400 mM mannitol, 40% (w/v) polyethylene glycol 6000 and 100 mM Ca(NO₃)₂), placed on ice for 20 min, and diluted into dilution solution (400 mM mannitol, 125 mM CaCl₂, 5 mM KCl, 5 mM glucose and 1.5 mM MES-KOH, pH 5.7). Protoplasts were collected and resuspended in MS medium supplemented with 400 mM mannitol and incubated with gentle rotation at 23°C for approximately 16 hours in the dark.

Confocal laser scanning microscopy

5-day-old thalli were used for observation unless otherwise defined. The samples were mounted in distilled water or dyeing solution and observed using an LSM 780 confocal microscope (Carl Zeiss) equipped with an oil immersion lens (63 \times , numerical aperture = 1.4) and an electrically driven stage. The samples were excited by laser at 488 nm (Argon 488) and 561 nm (DPSS 561-10), and the fluorescent emission was collected between 482-659 nm using twenty GaAsP detectors. Spectral unmixing, processing of the obtained images, and the construction of maximum intensity projection images were conducted using ZEN2012 software (Carl Zeiss). The images were processed digitally with ZEN2012 software and Photoshop software (Adobe Systems). For 4,4-difluoro-1,3,5,7,8-pentamethyl-4-bora-3a,4a-diaza-*s*-indacene (BODIPY 493/503, Thermo Fisher) staining, thalli or gemmae were incubated in 200 nM BODIPY 493/503 dissolved in water for 10 min. For *N*-(3-triethylammoniumpropyl)-4-(6-(4-(diethylamino)phenyl)hexatrienyl) pyridinium dibromide (FM4-64, Thermo Fisher) staining, thalli were soaked in 10 μ M FM4-64 solution for 2 min. Samples were then washed twice before observation. For observation by semi-super resolution microscopy, LSM 880 with Airy scan (Carl Zeiss) equipped with an oil immersion lens (63 \times , numerical aperture = 1.4) was used. The acquisition and calculation of images were conducted using ZEN 2 software (Carl Zeiss).

Electron microscopy

For the immunoelectron microscopic observation, 5-day-old Tak-1 thalli and the plant expressing mCitrine-MpSYP12B were used. The samples were fixed with 4% (w/v)

paraformaldehyde (PFA), 0.1% (w/v) glutaraldehyde (GA) (Distilled EM grade; Electron Microscopy Sciences, Hatfield, PA) and 0.5% (w/v) tannic acid in 0.05 M cacodylate buffer pH 7.4 at 4°C for 90 min, and then they were washed 3 times in 0.1 M cacodylate buffer for 15 min each. The samples were dehydrated in graded ethanol solutions (50% (v/v) and 70% (v/v)) at 4°C for 30 min each. The samples were infiltrated with a 50:50 mixture of ethanol and resin (LR white; London Resin Co. Ltd., Berkshire, UK) for 30 min each 3 times. After this infiltration, samples were incubated in 100% LR white three times at 4°C for 30 min each. The samples were transferred to a fresh 100% resin, and were polymerized at 50°C overnight. The polymerized resins were ultra-thin sectioned at 80 nm with a diamond knife using an ultramicrotome (Ultracut UCT; Leica, Vienna, Austria) and the sections were mounted on nickel grids. The grids were incubated with the primary antibody (rabbit polyclonal GFP pAb) in phosphate buffered saline (PBS) containing 1% (w/v) bovine serum albumin (BSA) at 4°C overnight, then they were washed with PBS plus 1% (w/v) BSA 3 times for 1 min. They were subsequently incubated with the secondary antibody conjugated to 10 nm gold particles (goat anti rabbit IgG pAb) for 1 hour at room temperature. And after washing with PBS, the grids were placed in 2% (w/v) GA in 0.1 M cacodylate buffer. Afterwards, the grids were dried and then were stained with 2% (w/v) uranyl acetate for 15 min and in Lead stain solution (Sigma-Aldrich Co., Tokyo, Japan) at room temperature for 3 min. The grids were observed by a transmission electron microscope (TEM, JEM-1400Plus; JEOL Ltd., Tokyo, Japan) at an acceleration voltage of 80 kV. Digital images (2048 × 2048 pixels) were taken with a CCD camera (VELETA; Olympus Soft Imaging Solutions GmbH, Münster, Germany).

For morphological observation by a TEM, 5-day-old Tak-1 thalli were used. The

samples were fixed with 2% (w/v) PFA and 2% (w/v) GA in 0.05 M cacodylate buffer pH 7.4 at 4°C overnight. After the fixation, samples were washed 3 times with 0.05 M cacodylate buffer for 30 min each, and were postfixed with 2% (w/v) osmium tetroxide in 0.05 M cacodylate buffer at 4°C for 3 hours. The samples were dehydrated in graded ethanol solutions (50% (v/v), 70% (v/v), 90% (v/v), and 100% (v/v)). The schedule was as follows: 50% (v/v) and 70% (v/v) for 30 min each at 4°C, 90% (v/v) for 30 min at room temperature, and 4 times of 100% for 30 min each at room temperature. After these dehydration processes, the samples were continuously dehydrated in 100% ethanol at room temperature overnight. The samples were transferred to a fresh 100% resin, and were polymerized at 60°C for 48 hours. The polymerized samples were ultra-thin sectioned at 70 nm with a diamond knife using an ultramicrotome (Ultracut UCT) and the sections were mounted on copper grids. They were stained with 2% (w/v) uranyl acetate at room temperature for 15 min, and then they were washed with distilled water followed by being secondary-stained with Lead stain solution (Sigma-Aldrich) at room temperature for 3 min. The grids were observed with a TEM (JEM-1400Plus) at an acceleration voltage of 80 kV. Digital images (2048 × 2048 pixels) were taken with a CCD camera (VELETA).

Lightsheet microscopy

5-day-old thalli expressing 2×Citrine driven by the Mp*SYPI2B* promoter were used for observation. The samples were embedded in low melt agarose gel and were observed using an Lightsheet Z.1 microscope (Carl Zeiss) equipped with a water immersion lens (5×, numerical aperture = 0.16). The samples were excited by laser at 488 nm (Argon 488). Acquisition of images and construction of three-dimension images from

multi-angle images were carried out using ZEN2014 software (Carl Zeiss). The images were processed digitally with Imaris software (Bitplane) and Photoshop software (Adobe Systems).

Thermal asymmetric interlaced-PCR (TAIL-PCR) and sequencing of TAIL-PCR products

TAIL-PCR was performed to identify flanking sequences of transfer DNA (T-DNA) insertions according to Liu *et al.*, 1995; Ishizaki *et al.*, 2008; Proust *et al.*, 2016 with minor modifications. Crude-extracted DNA was used as a template, flanking sequences were amplified using KOD FX neo DNA polymerase (Toyobo) and T-DNA-specific primers (TR1–3 and TL1–3 for the right border and the left border of T-DNA, respectively) and universal adaptor primers (AD1–6). The reaction cycles were shown in Table 2-2. After electrophoresis of the final TAIL-PCR products, bands were excised and DNA was purified from agarose gel using Wizard SV Gel and PCR Clean-Up System (Promega). Purified products were directly sequenced using TR3 or TL3 primer.

Table 2-1. The list of oligonucleotides used in the study.

Purpose	Gene name	primer 1 (5' to 3')	primer 2 (5' to 3')
RT-PCR	MpSYP8	CACCATGGCTACTGCCAAGGATGTAAC	TTATTGATACCAGTCCAAAAAC
	MpSYP3	CACCATGCCGGTGGCTCTGGGATCAGC	TCATGCTACGAAAACAACGAAAATTAAC
	MpSEC20	CACCATGGATCAAGATGTAGAAGAAGC	TTAGAGTTCATCATTTGATTGGTAC
	MpMEMB1	CACCATGGCGATGATGGGGAGCG	CTATCCACGGGCCCATCTCC
	MpGOS11	CACCATGGCAGTTGCGAATGGCTG	CTATTTGATATCCAGTACATG
	MpGOS12.1	ATGGAGGATGCGGACCCCGATGGG	CTATCTTCTGCGTCCGTTCCGATATCC
	MpGOS12.2	ATGGAGGATGCGGACCCCGATGGG	GTCAACGAGCATGAAGGGTGC
	MpUSE1A	CACCATGGGAATTTTCGAAGCGGAAG	CTAACCAGTGAGCCTTATCAAC
	MpUSE1B	CACCATGATACTTAGTAGAGCAGAG	TCAAGTGAGACGAATAATGAC
	MpBET1	CACCATGATGAACACTCGCCGAG	TCACTTTGTCAAGTAGTAAAC
	MpSFT1	CACCATGGCCAAGGGATCGAAGAGC	TTATCTAAGGAATTTAGCCC
	MpSEC22	CACCATGGTTAAATTAACCATTATTGC	TCAGCCGAAAATGTATCGC
	MpSYP4	CACCATGGCGACGCGCAATCAGACCG	TCAGAATAGAATTTTCTTCATGATATAC
	MpSYP2	CACCATGAGTTTTTTAGATCTAGAGG	TCACGCAAACATGACGATGATG
	MpVT11	CTGTCTCGGAAATGTACATCCACC	CACCAATGATCCCTCCCATGATCC
	MpSYP6A	CACCATGTCCGGCTTTAGATCCGTTTTAC	CTAGGCATTGAAAACAAGATAGGT
	MpSYP6B	CACCATGTGCATCTCGATCCTTATTATC	TCAAGTGTAATAATCAGCATG
	MpSYP5	CACCATGGCGCAAGCGGCGTCCG	TTACAAGGATTTGACCAAGC
	MpYKT6	CACCATGAAGATTACGGCCATTCTCC	TCACAATATCGAACAACTGG
	MpVAMP71	CACCATGGCTATTTTATATGCGCTC	TTAAGAGTGGCAGCCATACAAG
	MpSYP12A	CACCATGAACGATCTTCTGCAGAAAACG	CTACTTCTTCAAACTCGTAGCTATG
	MpSYP12B	CACCATGAACGATCTGCTGGCAAG	TCACTTTGCCGTTGCAATGATGG
	MpSYP13A	CACCATGAACGATCTTTTAGGGGAG	TCATGCTTTGTTTTGTTTTCCAAG
	MpSYP13B	CACCATGAACGATCTTCTGGGAGACTC	TCACTTTTGCCAGGGCTTGACG
	MpSNAP	CACCATGACCTCCGTGCATAGTAACC	TTATCGGTGGATGAGTCGTCGTG
	MpNPSN1	CACCATGGCCTCCCAAGGTCCCAG	CTAGGACTCCAACAAGCGAG
	MpSYP7A	CACCATGAGTGTTATAGATATCTTGAC	TCAGGCCAATAATTTGTATAG
	MpSYP7B	CACCATGAGCGTTACAGACTTGC	CTAGAAGAATTGATCTCCGAAG
	MpVAMP72A	CACCATGGGTGTGAACTCGTTGATTTAC	TTACTTGCACTTAAATCCCTTGC
	MpVAMP72B	CTACTGCTTCGTGGCTCGAGGAACGG	CGCCGACCGCCGGGAGGAGCAGTGCC
	MpVAMP72C	GTCACGTACACACGCGACGCCACACC	GATTACAAGATGAGCTTGATTACAAGCG
	MpVAMP72D	GGTGGTGTAGCGGAGTACAAGCCG	CGCCAAGTTGGCCAGAATCTCGGC
	MpVAMP72E	CACCATGGGGGCGAATCTTAGCAG	CTATATTGCAGTTTTAGCTTTTAG
	MpTOMOSYN11	GTACAGATTGTTGCGTCTTTACGC	CATTTCCATTACACTCGACACCTCC
	MpTOMOSYN12	CACCATGTGTCTTACTGGCCGCTCC	TCACAGCTCGTACCACTTCTCTG
	CUFF.11493	CGTGCCTCACGTCGGAATCTGATC	CTGGACATGGAGCTCAGCTTCGGG
	CUFF.21491	CACCATGCCTAGGACAATTGAAGTTGCC	TCATTCCCCCCTACATTGCACGAAC
	MpEF1 α	TCACTCTGGGTGTGAAGCAGATGA	GCCTCGAGTAAAGCTTCGTGGTG

Table 2-1. (continued)

Purpose	Gene name	primer 1 (5' to 3')	primer 2 (5' to 3')
pENTR for CDS	MpSYP8	CACCATGGCTACTGCCAAGGATGTAAC	TTATTGATACCAGTCCAAAAAC
	MpSYP3	CACCATGCCGGTGGCTCTGGGATCAGC	TCATGCTACGAAAACAACGAAAATTAAC
	MpSEC20	CACCATGGATCAAGATGTAGAAGAAGC	TTAGAGTTCATCATTGATTGGTAC
	MpMEMB1	CACCATGGCGATGATGGGGAGCG	CTATCCACGGGCCCATCTCC
	MpGOS11	CACCATGGCAGTTGCGAATGGCTG	CTATTTGATATCCAGTACATG
	MpGOS12.1	CACCATGGAGGATGCGGACCCCGG	CTATCTTCTGCGTCCGTTCCG
	MpGOS12.2	CACCATGGAGGATGCGGACCCCGG	TCACTTGGAATCCAGTAAAC
	MpUSE1A	CACCATGGGAATTTTCGCAAGCGGAAG	CTAACCAGTGAGCCTTATCAAC
	MpUSE1B	CACCATGATACTTAGTAGAGCAGAG	TCAAGTGAGACGAATAATGAC
	MpBET1	CACCATGATGAACACTCGCCGAG	TCACTTTGTCAAGTAGTAAAC
	MpSFT1	CACCATGGCCAAGGGATCGAAGAGC	TTATCTAAGGAATTTAGCCC
	MpSEC22	CACCATGGTTAAATTAACCATATTTC	TCAGCCGAAAATGTATCGC
	MpSYP4	CACCATGGCGACGCGCAATCAGACCG	TCAGAATAGAATTTCTTCATGATATAC
	MpSYP2	CACCATGAGTTTTTTAGATCTAGAGG	TCACGAAACATGACGATGATG
	MpVTI1	CACCATGTCTGAGATATTGGAAGGC	CTACTTACTACGACTGCTG
	MpSYP6A	CACCATGTCTGGCTTTTAGATCCGTTTTAC	CTAGGCATTGAAAACAAGATAGGT
	MpSYP6B	CACCATGTCTGCATCTCGATCCTTATTATC	TCAAGTGTAATAATCAGCATG
	MpSYP5	CACCATGGCGCAAGCGGCGTCGG	TTACAAGGATTTGACCAAGC
	MpYKT6	CACCATGAAGATTACGGCCATTCTCC	TCACAATATCGAACAACTGG
	MpVAMP71	CACCATGGCTATTTTATATGCGCTC	TTAAGAGTGGCAGCCATACAAG
	MpSYP12A	CACCATGAACGATCTTCTGCAGAAAACG	CTACTTCTTCAAACTCGTAGCTATG
	MpSYP12B	CACCATGAACGATCTGCTGGCAAG	TCACTTTGCCGTTGCAATGATGG
	MpSYP13A	CACCATGAACGATCTTTTAGGGGAG	TCATGCTTTGTTTGTTCCTCAAG
	MpSYP13B	CACCATGAACGATCTTCTGGGAGACTC	TCACTTTTGCCAGGGCTTGACG
	MpSNAP	CACCATGACCTCCGTGCATAGTAACC	TTATCGGTGGATGAGTCGTCTGTG
	MpNPSN1	CACCATGGCCTCCCAAGGTCCCGAG	CTAGGACTCCAACAAAGCGAG
	MpSYP7A	CACCATGAGTGTTATAGATATCTTGAC	TCAGGCCAATAATTTGTATAG
	MpSYP7B.1	CACCATGAGCGTTACAGACTTGC	TCATAAACGGAAGATCAAATTC
	MpSYP7B.2	CACCATGAGCGTTACAGACTTGC	CTAGAAGAATTGATCTCCGAAG
	MpVAMP72A	CACCATGGGTGTGAACTCGTTGATTTAC	TTACTTGCACTTAAATCCCTTGC
	MpVAMP72B	CACCATGGGGCGAAGAATGGC	TCACAGGAGGCGCCGACCGC
	MpVAMP72C	CACCATGGGATCGATTCTTAGCAG	TCATAAAAAATCTATACAACTTTTG
	MpVAMP72C ^{G2A}	CACCATGGCATCGATTCTTAGC	TCATAAAAAATCTATACAACTTTTG
	MpVAMP72D	CACCATGGGAGCGATTCTTAGCAG	CTAAAAATTTATACAAGGTTAC
	MpVAMP72D ^{G2A}	CACCATGGCAGCGATTCTTAGC	CTAAAAATTTATACAAGGTTAC
	MpVAMP72E	CACCATGGGGCGAATCTTAGCAG	CTATATTGCAGTTTTAGCTTTTAG
	MpVAMP72E ^{G2A}	CACCATGGCGGCGAATCTTAGC	CTATATTGCAGTTTTAGCTTTTAG
	MpTOMOSYN11	CACCATGTTTATCAAGCGGTTCTTCAG	TCAAAGTTCCCACCACTTCTTTGC
	MpTOMOSYN12	CACCATGTGTCTTACTGGCCGCTCC	TCACAGCTCGTACCACTTCTCTG
	MpCLC	CACCATGGCGGAGTTCGAGTATGGGG	GGCAGTCACAGCTGCTGCCGC

Table 2-1. (continued)

Purpose	Gene name	primer 1 (5' to 3')	primer 2 (5' to 3')	
pENTR for transient expression in <i>A. thaliana</i> cells	MpVAMP72A	GGCAAGCTTAAGGGTGGGCGCGCCG ACCCAG	GGCAAGCTTCTCTGCCAGCACGACA GTACCTC	
	MpVAMP72B	GGCAAGCTTAAGGGTGGGCGCGCCG ACCCAG	GGCAAGCTTCACTCCCGCCCCGTT CCTCGAG	
	MpVAMP72C	GGCAAGCTTAAGGGTGGGCGCGCCG ACCCAG	GGCAAGCTTCAAGCCATTCTTCGCC CGGGGCGAAGAATGGCTTGATCTAC TGCTAAGAATCGATC	
	MpVAMP72C ^{G2A}	GGCAAGCTTAAGGGTGGGCGCGCCG ACCCAG	GGCAAGCTTCAAGCCATTCTTCGCC CGGGGCGAAGAATGGCTTGATCTAC TGCTAAGAATCGATC	
	MpVAMP72D	GGCAAGCTTAAGGGTGGGCGCGCCG ACCCAG	GGCAAGCTTCAAGCCATTCTTCGGC CCGGGC	
	MpVAMP72D ^{G2A}	GGCAAGCTTAAGGGTGGGCGCGCCG ACCCAG	GGCAAGCTTCAAGCCATTCTTCGGC CCGGGC	
	MpVAMP72E	GGCAAGCTTAAGGGTGGGCGCGCCG ACCCAG	GGCAAGCTTGATCAAGTGATTCTTC ACATCG	
	MpVAMP72E ^{G2A}	GGCAAGCTTAAGGGTGGGCGCGCCG ACCCAG	GGCAAGCTTGATCAAGTGATTCTTC ACATCG	
	pENTR for genomic sequences	MpSYP12A 5'	GCAGGCTCCGCGGCCAAATTTAATA CTTATAGATTTG	GTGAAGGGGGCGGCCCTTTGGCAGAT CACTCCACCGTTG
		MpSYP12A CDS+3'	CACCCCCGGGGCAGCGGCATGAAC GATCTTCTGCAGAAAAC	AAGTGATTTCAATGTATGTCCCTC
MpSYP12B 5'		GCAGGCTCCGCGGCCTCTGTACTTG CATTTAGAAAATC	GTGAAGGGGGCGGCCACTGCTAAG CACAGAGTCGCAG	
MpSYP12B CDS+3'		CACCCCCGGGGCAGCGGCATGAAC GATCTGCTGGCAAGAG	ATCAGCCCCCGCGACGACAG	
MpSYP13A 5'		GCAGGCTCCGCGGCCAATTAGCAGA TCCAGCTGCTTCC	GTGAAGGGGGCGGCCGATTGCCGCC TGCTTGGCTTACTG	
MpSYP13A CDS+3'		AAGAAGGGTGGGCGCATGAACGATC TTTTAGGGGTATG	GCTGGGTCGGCGCGCAGATGTGACA AGGTCAAGAAGAAC	
MpSYP13B 5'		GCAGGCTCCGCGGCCGATCATGGCG AGTGTGTCGTGC	GTGAAGGGGGCGGCCGATTGCGCGC TGCTGCTGCCTCC	
MpSYP13B CDS+3'		CACCGGATCCGGCGGCAGCGGCATG AACGATCTTCTGGGAGACTC	CATACAACCTCAAACAATTTTGATG	
MpSYP2 5'		GCAGGCTCCGCGGCCACGAGCGAG TGAGACACCAGAGGAG	GTGAAGGGGGCGGCCCTCTGCTT CGTGGTAAATCCTCTTC	
MpSYP2 CDS+3'		CACCCCCGGGGCAGCGGCATGAGT TTTTTAGATCTAGAGGC	GCAAGTGGTGATGAGCCTTGCGTGC	
mCitrine-SmaI		GCCCCCTTACCCCCATGGTGAGCA AGGGCGAGGAG	CATGCCGCTGCCCCCTTGATACAGC TCGTCCATGCC	
mCitrine-BamHI		CCCCTTACCGGATCATGGTGAGCA AGGGCGAGGAG	GCTGCCGCGGATCCCTTGATACAGC TCGTCCATGCC	

Table 2-1. (continued)

Purpose	Gene name	primer 1 (5' to 3')	primer 2 (5' to 3')
gRNA	MpSYP12A	CTCGAGAAAGACACGACGGAGTCA	AAACTGACTCCGTCGTGTCTTTCT
	gRNA2		
	CUFF.11493	CTCGGCCGCTTCTCCACCATCGT	AAACACGATGGTGGAGAAGGCGGC
gRNA1			
	CUFF.11493	CTCGGTCAAATATATGTCTGGTAA	AAACTTACCAGACATATATTTGAC
	gRNA4		
Gateway vectors	proMpSYP12A:	GGCCAGTGCCAAGCTAAATTTAATACTT	TTTGTACAAACTTGTCTTGTACAGCTC
	mCitrine	ATAGATTTG	GTCCATGCCG
	proMpSYP12B:	GGCCAGTGCCAAGCTTCTGTACTTGCAT	TTTGTACAAACTTGTCTTGTACAGCTC
	mCitrine	TTAGAAAATC	GTCCATGCCG
	proMpCYCB1:	GGCCAGTGCCAAGCTGAGGATGGTTTAA	TTTGTACAAACTTGTCTTGTACAGCTC
	mCitrine	TCCTTTTTGC	GTCCATGCCG
Genotyping	CUFF.11493	CTTGCTAACAACTGAGAAGCTGG	CATGTTCAATGATTATACTCACCTC
	a-b		
	CUFF.11493	CTGCCGTCATGCGATCTCGCTCGG	GATGCTTGGATACGCAGTTGGTCG
c-d			
	CUFF.21491	CACCATGCCTAGGACAATTGAAGTTGCC	TCATTCCCCCTACATTGCACGAAC
	e-f		
TAIL-PCR	AD1	NGTCGASWGANAWGAA	
	AD2	TGWNAGSANCASAGA	
	AD3	AGWGNAGWANCAWAGG	
	AD4	GTNCGASWCANAWGTT	
	AD5	NTCGASTWTSWGTT	
	AD6	WGTGNAGWANCANAGA	
	TR1	CCTGCAGGCATGCAAGCTTGG	
	TR2	GCTGGCGTAATAGCGAAGAGG	
	TR3	CCTGAATGGCGAATGCTAGAG	
	TL1	CAGATAAGGGAATTAGGTTCCCTATAGG	
	TL2	TATAGGGTTTCGCTCATGTGTTGAGC	
	TL3	AGTACATTAAAAACGTCCGCAATGTG	

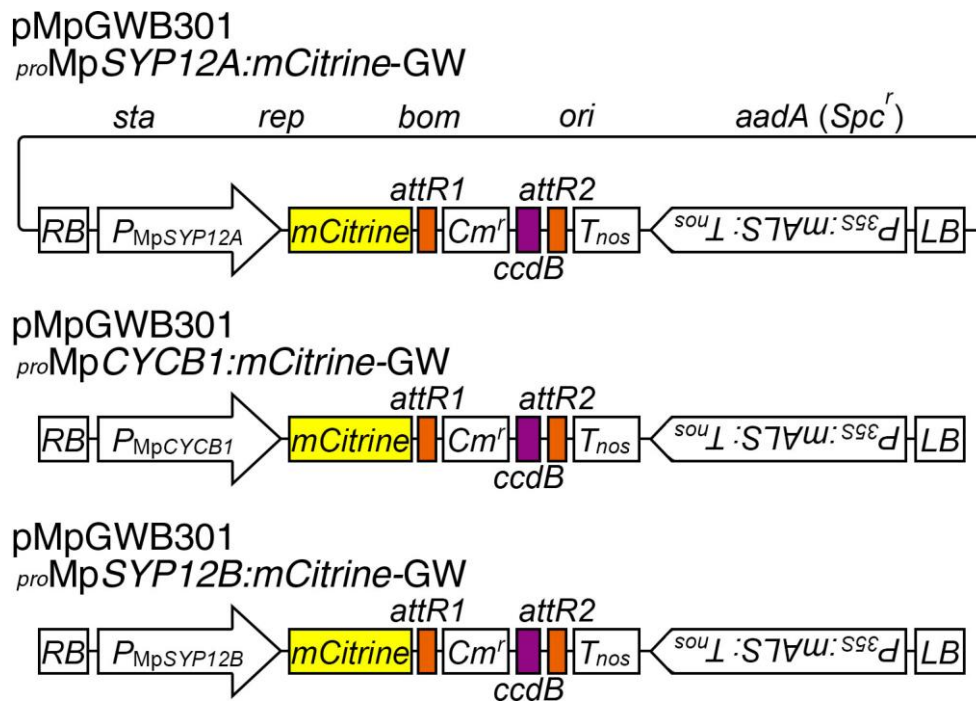


Figure 2-1. Gateway constructs

Schematic structures of gateway constructs prepared in this study. The vectors are derived from pMpGWB301 (Ishizaki *et al.*, 2015).

Table 2-2. Cycle setting for TAIL-PCR

Reaction	Cycle No.	Thermal settings
Primary	1	94°C 1 min, 95°C 1 min
	5	94°C 1 min, 65°C 1 min, 68°C 3 min
	1	94°C 1 min, 30°C 1min Ramping to 68°C 3 min, 68°C 3 min
	13	94°C 30 sec, 68°C 4 min 94°C 30 sec, 68°C 4 min 94°C 30 sec, 44°C 1 min, 68°C 3min
	1	68°C 5 min
	Secondary	1
13		94°C 30 sec, 68°C 4 min 94°C 30 sec, 68°C 4 min 94°C 30 sec, 44°C 1 min, 68°C 3 min
1		68°C 5 min
Tertiary		1
	13	94°C 30 sec, 68°C 4 min 94°C 30 sec, 68°C 4 min 94°C 30 sec, 44°C 1 min, 68°C 3 min
	1	68°C 5 min

Chapter III: Characterization of SNARE molecules of *Marchantia polymorpha*

Introduction

Membrane trafficking pathways and functions of organelles have been diversified among eukaryotic lineages, likely to fulfill functions specific to each lineage and/or organism, even though the basic molecular framework is highly conserved throughout eukaryotes. Completion of genome sequencing of Archaeplastida such as *Arabidopsis thaliana* (Arabidopsis Genome, 2000), *Populus trichocarpa* (Tuskan *et al.*, 2006), *Oryza sativa* (International Rice Genome Sequencing, 2005), *Selaginella moellendorffii* (Banks *et al.*, 2011), *Physcomitrella patens* (Rensing *et al.*, 2008), *Klebsormidium flaccidum* (Hori *et al.*, 2014), *Chlamydomonas reinhardtii* (Merchant *et al.*, 2007), *Ostreococcus tauri* (Palenik *et al.*, 2007), *Cyanidioschyzon merolae* (Matsuzaki *et al.*, 2004; Nozaki *et al.*, 2007), and many organisms of non-plant systems has enabled us to estimate and compare the complexity of the membrane trafficking system by counting numbers of machinery components of membrane trafficking such as Rab GTPases and SNARE molecules encoded in their genomes, which has provided insights into diversification and specification of membrane trafficking during eukaryotic evolution (Rutherford & Moore, 2002; Dacks & Field, 2007; Sanderfoot, 2007; Elias, 2008; Elias *et al.*, 2012).

In the green plant lineage, association between diversification of post-Golgi trafficking pathways and terrestrialization and/or multicellularization has been pointed out, which is based on increased numbers of genes for Rab GTPase, tethers, and SNARE proteins in land plants compared with algal species (Rutherford & Moore, 2002; Sanderfoot, 2007; Vukasinovic & Zarsky, 2016). Consistently, the evidence of unique

diversification of the post-Golgi trafficking system in plants has been obtained from studies using *A. thaliana* and tobacco. For example, the plant *trans*-Golgi network (TGN) has distinct functions from the TGN in animal cells; the TGN acts as the early endosome as well as functioning as a sorting hub in the secretory pathway in plant cells (Richter *et al.*, 2009; Uemura, 2016). The vacuolar transport is also organized in a plant-unique way, which acts as a fundamental basis of plant-specific vacuolar functions (Ebine *et al.*, 2014; Uemura & Ueda, 2014). Nevertheless, it is still possible that the increase in number of the machinery components reflects expansion of genes without functional differentiation because of recent whole or large-scale genome duplication, which is reported in several plant species (Tang *et al.*, 2008; Barker *et al.*, 2009). Thus, to gain more precise information on functional diversification of membrane trafficking during plant evolution, analyses in basal plant lineages including bryophytes and algal species are apparently needed.

To gather information regarding evolution and diversification of the membrane trafficking pathways in plants, I systematically analyzed SNARE molecules in the liverwort, *Marchantia polymorpha*. I identified 34 genes for SNARE proteins in *M. polymorpha* and subcellular localization of the majority of these SNARE molecules by expressing fluorescently tagged proteins in *M. polymorpha* thallus cells. The comparison of the subcellular localization of orthologous products between *M. polymorpha* and *A. thaliana* indicated that the membrane trafficking system has increased its complexity during land plant evolution, although *M. polymorpha* also seems to acquire specialized trafficking pathways unique to the organism.

Results

Genes for SNARE proteins encoded in the *M. polymorpha* genome

To gather information about the diversification of membrane trafficking pathways during the evolution of land plants, I comprehensively analyzed SNARE molecules in the liverwort *M. polymorpha*. I searched genes for proteins with the SNARE motif from the genome and transcriptome databases of *M. polymorpha* and discovered that 37 SNARE proteins in 34 loci were encoded in the *M. polymorpha* genome (Figure 3-1). These proteins were classified into 5 groups: 8 Qa-SNAREs, 7 Qb-SNAREs, 10 Qc-SNAREs, 1 Qb+Qc-SNARE, and 11 R-SNAREs. The majority of the SNARE genes in *M. polymorpha* lack paralogs in the genome, except MpGOS1, MpUSE1, MpSYP6, MpSYP1, MpSYP7, MpVAMP72, and MpTOMOSYN1 (Figure 3-1). Homologs of all SNARE genes in *M. polymorpha* were also found in other land plants with a greater degree of redundancy, while the SYP1 group was multiplied also in *M. polymorpha*. Four SYP1 genes were found in the genome of *M. polymorpha*, two each of which were categorized into the SYP11/12 and SYP13 groups. The phylogenetic analysis estimated that the SYP1 group of the green plants is divided into two major groups: chlorophyte SYP1 and streptophyte SYP1, furthermore the SYP1 group of streptophytes is separated into two major groups: SYP13 and SYP11/12 groups (Figure 3-1 and 3-2). Among SYP11/12 group, SYP11 and SYP12 subgroups could diverge at the emergence of seed plants, and lycophytes and bryophytes including *M. polymorpha* possess the ancestral class of the SYP11/12 members (Figure 3-2). Each SYP1 member of *M. polymorpha* typically possessed a syntaxin domain, a Qa-SNARE domain, and a transmembrane domain (TMD), and these four SYP1 members were highly similar in their primary sequences aligned (Figure 3-3).

Splicing variants were detected for three loci, *MpSYP7B*, *MpVAMP72A*, and *MpGOS12*. Two splicing variants at the *MpSYP7B* locus were amplified by RT-PCR; *MpSYP7B.1* encoded a canonical Qc-SNARE protein comprising of a syntaxin domain, a Qc-SNARE domain, and a TMD, while the protein translated from the other transcript, *MpSYP7B.2* lacked the TMD (Figure 3-4A). Two different transcripts were amplified from the *MpVAMP72A* locus with a consequence of alternative splicing. Each R-SNARE protein translated from the transcripts contained a longin domain, an R-SNARE domain, and a TMD, which R-SNARE proteins were comprised of different lengths of the longin domains (Figure 3-4B). Based on the transcriptome information, two different length of transcripts were amplified from the *MpGOS12* locus. Both transcripts were predicted to be translated into Qb-SNARE proteins containing a Qb-SNARE domain and a TMD, with differences in the lengths of the carboxyl termini (Figure 3-4C).

Next, I examined the transcription profiles of the SNARE genes by RT-PCR in different developmental organs using *MpEF1 α* as a standard, the mRNA levels of which exhibit a constant accumulation in various tissues and under several environmental-stress conditions examined to date (Althoff *et al.*, 2013; Kanazawa *et al.*, 2013). Most of the SNAREs were ubiquitously transcribed in all of the demonstrated organs [5-day-old thalli, antheridiophores (male reproductive organs), archegoniophores (female reproductive organs), and 7-day-old sporelings], while several genes were detected to be transcribed in specific organs (Figure 3-5). One of the transcript variants at *MpGOS12* locus, *MpGOS12.2*, was detected only in thalli. *MpUSE1B* was transcribed in antheridiophores, archegoniophores, and sporelings but not in thalli, and the transcripts of both *MpSYP6B* and *MpSYP7B* were detected only in antheridiophores. Both *MpSYP12B* and *MpTOMOSYN12* were transcribed in thalli, antheridiophores, and archegoniophores but

not in sporelings. The transcripts of MpVAMP72E were detected in thalli, archegoniophores, and sporelings but not in antheridiophores. I could not detect the transcripts of MpVAMP72D in any organs under the experimental condition. These results indicate that the genes without their paralogs are constitutively expressed in *M. polymorpha* plants during all developmental stages, in contrast several genes with their paralogs exhibit organ-specific transcription profiles, probably reflecting specific and/or additional requirements for development of specific cells.

Novel VAMP72 members with characteristic structures in *M. polymorpha*

In addition to the basal set of SNARE molecules that are conserved among land plants (Figure 3-1), I identified three VAMP72 members, with unique structures. VAMP7 belongs to the longin-type R-SNAREs. The longin domain of VAMP7 is usually positioned at the N-terminus followed by an R-SNARE domain and a TMD. In addition to these canonical three domains, MpVAMP72C, MpVAMP72D, and MpVAMP72E possessed extended sequences comprising 12-14 amino acid residues at their N-termini, which were predicted to contain the consensus sequence for *N*-myristoylation (predicted by NMT; <http://mendel.imp.ac.at/myristate/SUPLpredictor.htm> and Myristoylator; <http://web.expasy.org/myristoylator/>, Bologna *et al.*, 2004) (Figure 3-6A). R-SNARE proteins with potential *N*-myristoylation extension have not been reported to be identified in any other species, suggesting that this type of R-SNARE is uniquely acquired in liverworts. The other four VAMP7 proteins in *M. polymorpha*, MpVAMP71, two MpVAMP72A products derived from the same gene, and MpVAMP72B, did not contain the consensus for *N*-myristoylation. To verify whether the N-terminal sequences of MpVAMP72C–E were actually *N*-myristoylated in plant cells, I expressed the N-terminal

20 amino acids of MpVAMP72C–E tagged with enhanced yellow fluorescent protein (EYFP) in the protoplasts of *A. thaliana* cells cultured in suspension. The results showed that these chimeric proteins were localized to membrane vesicles, the endoplasmic reticulum (ER), and the plasma membrane (PM) (Figure 3-6B, D, and F). In contrast, the N-terminal 20 amino acid sequences of MpVAMP72A and MpVAMP72B and N-terminal sequences of MpVAMP72C–E, in which the glycine residue that was expected to undergo *N*-myristoylation was replaced with alanine (G2A), did not target EYFP to membranous compartments but revealed the dispersal of EYFP into the cytosol and nuclei (Figure 3-6C, E, G, H, and I). These results indicated that *M. polymorpha* possesses novel VAMP72 members that are *N*-myristoylated.

Markers of the Golgi apparatus and *trans*-Golgi network in *M. polymorpha*

To elucidate the functions of SNARE molecules, it is important and efficient to know their subcellular localization, and this endeavor should be preceded by the establishment of reliable organelle markers in *M. polymorpha*. To achieve this goal, I examined whether the Golgi marker used in *A. thaliana* and tobacco also works in *M. polymorpha*. Fluorescent proteins fused with the TMD of rat sialyltransferase (ST) are widely used as reliable Golgi markers (Boevink *et al.*, 1998; Ito, Y *et al.*, 2012). To verify whether the ST tagged with a fluorescent protein (XFP) is also useful in *M. polymorpha*, I expressed ST-Venus and ST-monomeric red fluorescent protein (mRFP) driven by the cauliflower mosaic virus (CaMV) 35S promoter in *M. polymorpha* thallus cells. These chimeric proteins were localized to punctate compartments in the cytoplasm and showed perfect overlap (Figure 3-7A). As a marker of the *trans*-Golgi network (TGN), I employed MpSYP6A because its orthologous product of *A. thaliana* is an established marker of the

TGN (Sanderfoot *et al.*, 2001a; Uemura *et al.*, 2004; Robert *et al.*, 2008; Choi *et al.*, 2013). Fluorescence from Citrine-MpSYP6A and mRFP-MpSYP6A driven by the CaMV 35S promoter and Mp*EFL* α promoter, respectively, was observed on punctate compartments and the PM with perfect overlap (Figure 3-7B and C). Immune-electron microscopy using a polyclonal anti-GFP antibody demonstrated that punctate compartments visualized by ST-Venus or Citrine-MpSYP6A were *trans* cisternae of the Golgi apparatus and the TGN, respectively, in transgenic *M. polymorpha* expressing ST-Venus or Citrine-MpSYP6A (Era, 2013). These results indicated that ST-XFP is also useful as a Golgi apparatus marker in *M. polymorpha* cells. Thus, ST-mRFP and mRFP-MpSYP6A can be used as markers of the Golgi apparatus and TGN in *M. polymorpha*, respectively. Most of the TGN was observed to be associated with the Golgi apparatus, but Golgi-independent TGN was also observed (arrowheads in Figure 3-7D and E). Similar Golgi-associated and Golgi-independent TGN have also been reported in *A. thaliana* (Viotti *et al.*, 2010; Uemura *et al.*, 2014), which suggests that the organization and function of the TGN are conserved at least partially among land plant lineages.

Subcellular localization of fluorescently tagged SNARE proteins in *M. polymorpha*

Next, I analyzed the subcellular localizations of major members of the SNARE family in *M. polymorpha* by expressing fluorescently tagged SNARE molecules under the control of the CaMV 35S or their own promoters. The subcellular localization of these molecules was classified into several categories.

ER- and Golgi apparatus-localized SNAREs

I identified at least six ER-localized SNAREs: Qa-MpSYP8, Qb-MpSEC20, Qc-MpUSE1A, Qc-MpUSE1B, Qc-MpSYP7B.1, and R-MpSEC22. Citrine-fused

MpSYP7B.1, MpSEC20, MpUSE1A, and MpSEC22 driven by the CaMV 35S promoter were localized to reticulated membrane tubules and cisternal structures that were connected to the tubules (Figure 3-8A–D), which is the typical structure of the ER in both plant and animal cells (Voeltz *et al.*, 2002; Borgese *et al.*, 2006). The fluorescence of Citrine-MpUSE1B was scarcely detected in the reticulated pattern; it was observed on the nuclear envelope almost exclusively (Figure 3-8E), which is continuous with the ER. Nuclear-envelope localization was also observed in cells expressing other fluorescently tagged ER-localized SNAREs (for example, see Figure 3-8D). Citrine-MpSYP8 was localized to numerous punctate membrane domains, which were independent of and smaller in size than the Golgi apparatus visualized using ST-mRFP (Figure 3-8F). The punctate domains could be subdomains of the ER, as previously described for tobacco leaf cells (Bubeck *et al.*, 2008). In a consistent manner, Citrine-MpSYP8 was also localized to the reticulated network occasionally in addition to small punctate domains associated with the network (asterisk in Figure 3-8F).

Seven SNARE proteins were localized to the Golgi apparatus: Qa-MpSYP3, Qb-MpMEMB1, Qb-MpGOS11, Qb-MpGOS12.1, Qb-MpGOS12.2, and Qc-MpSFT1, and R-MpTOMOSYN11. These proteins driven by the CaMV 35S promoter were observed only on punctate organelles in the cytoplasm in *M. polymorpha* thallus cells, in which these SNAREs colocalized or tightly associated with ST-mRFP (Figure 3-9A, C, E, G, I, K, and M). Conversely, colocalization was not observed between these SNAREs and the TGN marker, mRFP-MpSYP6A (Figure 3-9B, D, F, H, J, L, and N).

These ER- or Golgi-localized SNARE molecules should be involved in the membrane trafficking pathways between the ER and Golgi apparatus and/or around the Golgi apparatus, such as the intra-Golgi transport and retrograde transport from post-

Golgi organelles in *M. polymorpha*.

TGN-localized SNAREs

I identified six TGN-localized SNAREs: Qa-MpSYP4, Qb-MpVTI1, Qc-MpBET1, Qc-MpSYP6A, Qc-MpSYP6B, and R-MpVAMP72B. Citrine-fused MpSYP4, MpVTI1, MpBET1, and MpSYP6B driven by the CaMV 35S promoter were localized to punctate compartments in *M. polymorpha* thallus cells, which also bore mRFP-MpSYP6A, the TGN marker (Figure 3-10A, C, E, and G). ST-mRFP, the Golgi apparatus marker, was not colocalized with these SNARE members (Figure 3-10B, D, F, and H).

Vacuolar membrane-localized SNAREs

Qa-MpSYP2, Qc-MpSYP5, and R-MpVAMP71 were localized to the vacuolar membrane in *M. polymorpha* thallus cells. Citrine-fused MpSYP2 and MpSYP5 driven by the CaMV 35S promoter were observed exclusively on the vacuolar membrane (Figure 3-11A and B), and Citrine-MpVAMP71 was also localized to punctate compartments (Figure 3-11C and D). To identify the punctate compartments, I coexpressed Citrine-MpVAMP71 and ST-mRFP or mRFP-MpSYP6A in *M. polymorpha* plants, and I discovered that Citrine-MpVAMP71 did not colocalize with either marker, although they are frequently observed in a close proximity (Figure 3-11C and D). These punctate compartments might represent multivesiculated endosomes, which have been occasionally observed close to the Golgi and TGN in *A. thaliana* cells (Richter *et al.*, 2007; Scheuring *et al.*, 2011; Singh *et al.*, 2014), or adaptor protein complex 3 (AP-3)-positive compartments, which are responsible for the transport of VAMP713 in *A. thaliana* (Ebine *et al.*, 2014).

In transgenic plants expressing Citrine-fused vacuolar membrane SNAREs, spherical structures with a strong fluorescence intensity, which were referred to as bulbs in *A. thaliana* (Saito *et al.*, 2002), were frequently observed in vacuoles (Figure 3-12A, C, and D). It has recently been reported that overexpression and a weak dimerizing nature of GFP lead to artificial enhancement of the accumulation of bulbs in *A. thaliana* (Segami *et al.*, 2014). To eliminate potential artificial effects of overexpression and dimerization of the fluorescent protein fused to MpSYP2 in *M. polymorpha*, I constructed a chimeric gene consisting of the MpSYP2 promoter, the cDNA for monomeric Citrine (mCitrine) to which the mutation leading to monomerization of GFP variants (Segami *et al.*, 2014) was introduced, and the genomic sequence of MpSYP2 starting from the start codon. In *M. polymorpha* plants expressing mCitrine-MpSYP2 under the regulation of its own promoter, I did not observe bulb-like spherical structures in the vacuole (Figure 3-12B). This result strongly suggests that overexpression and/or dimerization of fluorescently tagged vacuolar membrane SNAREs also results in an artificial enhancement of bulb-like structure formation in *M. polymorpha*.

PM- and oil body membrane-localized SNAREs

I then focused my interest on SNARE molecules on the PM. A majority of SYP1 members have been localized to the PM in *A. thaliana*, whose numbers have been reported to expand drastically during land plant evolution (Sanderfoot, 2007). It has also been reported that SYP111/KNOLLE, which is responsible for cell plate formation in dividing cells (Lukowitz *et al.*, 1996), is mislocalized to the PM when expressed in non-dividing cells (Völker *et al.*, 2001). Thus, to collect information on the authentic localization and expression of SYP1 members in *M. polymorpha*, I expressed SYP1

members tagged with mCitrine under the regulation of their own regulatory elements including 5'- and 3'-flanking regions and introns. Qa-MpSYP12A, Qa-MpSYP13A, and Qa-MpSYP13B were mainly localized to the PM in almost all cells in thalli (Figure 3-13A–C). Intriguingly, Qa-MpSYP13A was also localized to the oil body membrane in oil body cells (Figure 3-13D), which are a unique development in liverworts. Furthermore, Qa-MpSYP12B was specifically expressed in oil body cells and was localized to the oil body membrane with faint localization on the PM (Figure 3-13E). Oil body cells, a liverwort-specific cell containing the oil body, were recognized as dark-colored cells in the low magnification bright field (BF) images (Figure 3-14). Oil body cells were detected in 5-day-old thalli, antheridiophores, and archegoniophores, whereas they were not observed in sporelings (Figure 3-14), which is consistent with the absence of the *MpSYP12B* transcript in sporelings, as demonstrated by RT-PCR (Figure 3-5). The oil body localization was not observed for the other MpSYP1 members (Figure 3-13F and G). These results indicate that the functions of SYP1 members have also diverged in *M. polymorpha*.

Regarding the SNARE molecules of subgroups other than Qa-SNAREs, I found that Citrine-tagged Qb-MpNPSN1 and R-MpVAMP72B were localized to the PM when they were expressed under the regulation of the CaMV 35S promoter (Figure 3-13H–J). Citrine-MpVAMP72B was also observed on punctate compartments, majority of which colocalized with the TGN marker, mRFP-MpSYP6A (Figure 3-13I). However, a part of the punctate compartments were independent of the TGN (arrowhead in Figure 3-13I), which could correspond to the intermediate compartments that are responsible for transport between the TGN and PM as reported in *A. thaliana* (Asaoka *et al.*, 2012). Colocalization between Citrine-MpVAMP72B and the Golgi marker, ST-mRFP, was not

observed (Figure 3-13J). Citrine-tagged Qb+Qc-MpSNAP, an *M. polymorpha* homolog of SNAP25, was dispersed into the cytosol following its expression under the regulation of the CaMV 35S promoter (Figure 3-13K). GFP-tagged orthologous products in *A. thaliana*, SNAP29, SNAP30, and SNAP33 were also shown to be dispersed into the cytosol in *A. thaliana* protoplasts (Uemura *et al.*, 2004), although these molecules mediate trafficking events to the PM, including a pathogen response (Kwon *et al.*, 2008) and cell plate formation (Heese *et al.*, 2001; El Kasmi *et al.*, 2013). Because the CaMV 35S promoter was inactive in the oil body cell (Figure 3-15), I could not verify the localization of Qb-, Qc-, and R-SNAREs on the oil body membrane.

Discussion

In Chapter III, I analyzed SNARE molecules in *M. polymorpha*, the genome of which is currently under detailed investigations. I showed that *M. polymorpha* has a conserved set of SNARE molecules with lower degrees of redundancy than the other land plant lineages. The genome of the moss *P. patens*, which also belongs to the bryophyte, encodes 57 SNARE proteins (Sanderfoot, 2007; Rensing *et al.*, 2008). This number is almost equivalent to the number of SNAREs in *A. thaliana*, which possesses 63 SNARE proteins (Sanderfoot, 2007). Conversely, smaller numbers of SNARE proteins are encoded in the genomes of unicellular algal species; 29 and 20 SNARE proteins have been identified in *C. reinhardtii* and *O. tauri*, respectively (Sanderfoot, 2007). Based on this evidence, it has been suggested that the expansion of the SNARE genes could be associated with the multicellularization and/or terrestrialization of green plants (Dacks & Field, 2007; Sanderfoot, 2007). However, my results and the recently unveiled genome of the filamentous charophytic algae, *K. flaccidum* (Hori *et al.*, 2014), did not firmly support this notion; the majority of the subgroups of SNARE protein in *M. polymorpha* consist of only one member that is expressed in all of the organs examined. Conversely, subgroups comprising two paralogous members, such as the MpGOS1, MpUSE1, MpSYP6, MpSYP7, and MpTOMOSYN1 groups, exhibited distinct expression patterns between the subgroup members; one was expressed ubiquitously and the other was expressed in an organ-specific manner. The subcellular localization of GOS1, USE1, and SYP6 groups with fluorescently tagged SNARE proteins also revealed that the paralogous gene products exhibited a similar subcellular localization when expressed under the CaMV 35S promoter (summarized in Figure 3-16); this was largely identical to the localization of the orthologous products in *A. thaliana* (Uemura *et al.*, 2004). These

results indicated that the duplication of SNARE genes followed by the differentiation of regulatory elements such as the promoter resulted in the differentiation of expression patterns without changing the subcellular localization and presumably the molecular function in these subgroups.

SNAREs with distinct subcellular distributions in *A. thaliana* and *M. polymorpha*

Although the subcellular localization of a majority of SNARE proteins in *M. polymorpha* was comparable with that of the orthologous products of *A. thaliana*, several SNARE proteins exhibited distinct behaviors between *A. thaliana* and *M. polymorpha* (Figure 3-16).

Early secretory SNAREs

Several SNARE molecules that function in early secretory organelles such as the ER and Golgi apparatus exhibited good conservation in terms of their subcellular localization among land plants. For example, a putative set of cognate SNAREs, Qa-SYP8, Qb-SEC20, Qc-USE1, and R-SEC22, which are counterparts of the SNAREs that mediate retrograde transport from the Golgi apparatus to the ER in budding yeast (Lewis & Pelham, 1996; Lewis *et al.*, 1997; Dilcher *et al.*, 2003; Hong, 2005), were also localized to the ER and related compartments in both *A. thaliana* (Uemura *et al.*, 2004) and *M. polymorpha* (this study). These results suggest that the functions of these molecules are conserved. Among the *M. polymorpha* SNARE molecules that are homologous to yeast SNAREs mediating anterograde transport from the ER to the Golgi apparatus (Qa-Sed5p, Qb-Bos1p, Qc-Bet1p, and R-Sec22p, Newman *et al.*, 1990; Hardwick & Pelham, 1992; Banfield *et al.*, 1995; Nichols & Pelham, 1998), MpSYP3 (homologous to Sed5) and

MpMEMB1 (homologous to Bos1p) were also localized to the Golgi apparatus. However, MpBET1 was predominantly localized to the TGN in *M. polymorpha*, exhibiting good colocalization with MpSYP6A (Figure 3-10G). Intriguingly, the *A. thaliana* BET1 homolog BET11/BS14a is localized to *trans* cisternae of the Golgi apparatus in *A. thaliana* cells cultured in suspension (Uemura *et al.*, 2004) and tobacco leaf epidermal cells (Chatre *et al.*, 2005). These results may indicate diversified functions of BET1 among land plant lineages, although the effects of XFP tagging and overexpression on subcellular localization should be verified in future studies.

I also noticed a slight difference in the subcellular localization of Qc-SYP7 members between *A. thaliana* s and *M. polymorpha*. The SYP7 group is plant-specific Qc-SNARE (Sanderfoot *et al.*, 2000), and the genome of *A. thaliana* encodes three SYP7 members (SYP71–73). GFP-fused SYP71 is predominantly targeted to the PM, with slight localization at the ER in meristematic cells, when it is expressed under the regulation of its own promoter (Suwastika *et al.*, 2008). The PM localization of SYP71 is further supported by fractionation and co-immunoprecipitation studies (Suwastika *et al.*, 2008; El Kasmi *et al.*, 2013). However, Citrine-tagged MpSYP7B.1 driven by the CaMV 35S promoter was localized to the ER in *M. polymorpha* thallus cells (Figure 3-8A). These distinct localization patterns are most likely explained by the sensitivity of the subcellular localization of SYP7 members to overexpression or ectopic expression. It has been reported that transient expression of fluorescently tagged *A. thaliana* SYP7 members in *A. thaliana* protoplasts and tobacco leaf cells results in localization at the ER (Uemura *et al.*, 2004; Wei *et al.*, 2013), which suggests that the expression level must be strictly regulated for the proper localization of SYP7. As indicated in Figure 3-5, MpSYP7B is not transcribed in thalli. However, I do not rule out the possibility that SYP7 members

also mediate membrane fusion at the ER in *M. polymorpha* (and also in *A. thaliana*). The occurrence of two Qc-SNAREs on the ER, MpUSE1 and MpSYP7, may represent the existence of two distinctive trafficking pathways to the ER. Further studies are needed to obtain complete information regarding the functions of the SYP7 group in land plants.

Vacuolar SNAREs

Qa-SYP2 represents the first group of SNAREs to be identified in plants and is known to act in vacuolar and endosomal trafficking pathways (Sanderfoot *et al.*, 1999; Sanderfoot *et al.*, 2000; Saito & Ueda, 2009). There are three *SYP2* genes in the genome of *A. thaliana* (*SYP21–23*). *SYP21/PEP12* and *SYP22/VAM3* were initially isolated as *A. thaliana* genes that rescue the deleterious effects of the yeast *pep12* and *vam3* mutations, respectively (Bassham *et al.*, 1995; Sato *et al.*, 1997), which suggests that the functions of the SYP2 members had already diverged in the common ancestor of yeasts and plants into the *SYP21/PEP12* and *SYP22/VAM3* groups. However, phylogenetic and comparative genomic analyses indicate that these genes diversified independently and convergently in fungal and plant lineages (Dacks *et al.*, 2008). In the present study, I found that *M. polymorpha* harbors only one *SYP2* member, supporting this notion. MpSYP2 resided on the vacuolar membrane, and no other Qa-SNAREs were localized to the vacuolar membrane. This result indicated that MpSYP2 is the sole vacuolar Qa-SNARE. In *A. thaliana*, *SYP21/PEP12* is predominantly localized to the prevacuolar compartment (PVC), whereas *SYP22/VAM3* is preferentially localized to the vacuolar membrane, although they have partially redundant functions (Sanderfoot *et al.*, 1999; Sanderfoot *et al.*, 2001b; Ohtomo *et al.*, 2005; Shirakawa *et al.*, 2010; Uemura *et al.*, 2010). A detailed comparison of MpSYP2 and SYP2 members of *A. thaliana* would

provide invaluable information on the diversification of the subcellular localization and functions of SYP2 members during plant evolution.

The Qb-VTI1 group would be another good target of study to unravel mechanisms underlying the functional diversification of SNARE proteins. There are four paralogous VTI1 proteins in *A. thaliana* (VTI11–14), which are diversified in their localization and functions. VTI11 is predominantly localized to the PVC and vacuolar membrane with a small population on the TGN in *A. thaliana* (Zheng *et al.*, 1999; Uemura *et al.*, 2004), and it mediates membrane fusion at the vacuole by forming a complex with SYP22/VAM3, SYP51, and VAMP727 or VAMP71 (Sanderfoot *et al.*, 1999; Zheng *et al.*, 1999; Sanderfoot *et al.*, 2001a; Yano *et al.*, 2003; Niihama *et al.*, 2005; Ebine *et al.*, 2008; Ebine *et al.*, 2011; Fujiwara *et al.*, 2014). Conversely, VTI12 is mainly localized to the TGN and PM (Uemura *et al.*, 2004; Niihama *et al.*, 2005), where it functions distinctly from VTI11 in vacuolar trafficking pathways and autophagy (Surpin *et al.*, 2003; Sanmartin *et al.*, 2007; Zouhar *et al.*, 2009) in a complex with SYP41, SYP51, and SYP61 (Bassham *et al.*, 2000; Sanderfoot *et al.*, 2001a; Niihama *et al.*, 2005; Zouhar *et al.*, 2009). In contrast, *M. polymorpha* harbors only one *VTI1* homolog. Intriguingly, Citrine-MpVTI1 was localized to the TGN almost exclusively in *M. polymorpha* thallus cells (Figure 3-10C). This result could indicate that ancestral *VTI1* acted centrally in membrane trafficking around the TGN, and paralogous expansion of *VTI1* genes followed by the accumulation of mutations led to the diversification of their subcellular localization, binding partners, and functions during land plant evolution.

A similar paralogous expansion in *A. thaliana* was also observed in the VAMP71 group, for which the *M. polymorpha* genome contains only one gene. Four VAMP71 members are encoded in the genome of *A. thaliana* (VAMP711–714), among which

VAMP711, VAMP712, and VAMP713 are exclusively localized on the vacuolar membrane (Carter *et al.*, 2004; Szponarski *et al.*, 2004; Uemura *et al.*, 2004; Uemura *et al.*, 2005; Geldner *et al.*, 2009; Ebine *et al.*, 2014). However, VAMP714 is also observed on the Golgi apparatus (Uemura *et al.*, 2004). VAMP714 is detected in the vacuolar membrane fraction (Szponarski *et al.*, 2004) and interacts with SYP22 in co-immunoprecipitation experiments (Fujiwara *et al.*, 2014). These results may suggest that VAMP714 functions during transport from the Golgi apparatus to the vacuole.

Different localization of SYP1 members in *M. polymorpha*

The Qa-SYP1 family is one of the most diversified SNARE families in land plants, especially in seed plants (Sanderfoot, 2007). For example, close homologs of SYP111/KNOLLE, which is expressed only in dividing cells and mediates membrane fusion at forming cell plates in *A. thaliana* (Lukowitz *et al.*, 1996; Lauber *et al.*, 1997; Enami *et al.*, 2009), are found only in seed plant lineages (Sanderfoot, 2007); however, cytokinesis involving cell plate formation is observed throughout land plant lineages and in some algal species (Pickett-Heaps, 1967; Marchant & Pickett-Heaps, 1973; McIntosh *et al.*, 1995; Chapman *et al.*, 2001; Cook, 2004; Katsaros *et al.*, 2011). In *M. polymorpha*, I did not identify a Qa-SNARE that was specialized for cell plate formation, although I found one of SYP1 members required for cell plate formation during cytokinesis in *M. polymorpha* thallus cells, which will be presented in the next chapter.

Three of four SYP1 members in *M. polymorpha*, MpSYP12A, MpSYP13A, and MpSYP13B, were expressed in the whole tissues of 5-day-old thalli, and MpSYP12B was only expressed in oil body cells (Figure 3-13). The oil bodies in liverworts, which are formed in liverwort-specific oil body cells, are responsible for the synthesis and storage

of specific isoprenoids, phenolics, and bisbibenzyl compounds such as marchantin and its relatives (Asakawa, 1983; Suire *et al.*, 2000; Asakawa *et al.*, 2013; Tanaka *et al.*, 2016). The oil body is surrounded by a single unit membrane, which is reported to originate from the ER cisternae (Duckett, 1995; Suire, 2000). Interestingly, my results demonstrated that the surface membrane of the oil body and the PM shared the common Qa-SNAREs. In the Chapter IV and V, detailed mechanisms underlying oil body formation and the involvement of membrane trafficking in this process will be further investigated.

A novel type of R-SNARE

In this study, I identified novel R-SNARE members with a distinctive structural characteristic. MpVAMP72C–E were classified in the VAMP72 group; however, these molecules harbor the consensus sequence for *N*-myristoylation in addition to functional domains constituting canonical VAMP7 members. I confirmed that the N-terminal sequences of these proteins are indeed *N*-myristoylated in *A. thaliana* cells. Thus, these *N*-myristoylated VAMP72 (Myr-VAMP72) proteins should be attached to the membrane at two sites in the polypeptides: the myristoylated N-terminus and the C-terminal TMD. To my best knowledge, this type of R-SNARE has not been identified in other organisms including plants, which indicates that this type of SNARE was uniquely acquired in the liverwort during evolution. It is anticipated that uniquely acquired SNARE molecules could be involved in distinctive membrane trafficking pathways, underlying the specialized functions of the liverwort. The subcellular localization, effect of knock-out mutations, and identification of binding partners of these Myr-VAMP72 proteins would also be interesting for future projects to unravel the molecular function and physiological significance of Myr-VAMP72 in *M. polymorpha*.

SNARE molecules with distinct but unique structures in terms of membrane binding domains have also been reported in other systems. Animal Syntaxin 17, which possesses two tandem TMD-like structures, has been shown to mediate membrane fusion between the autophagosome and lysosome (Itakura *et al.*, 2012), in addition to its function in trafficking between the ER and ER-Golgi intermediate compartment (Stegmaier *et al.*, 2000; Muppirala *et al.*, 2011). SNARE molecules with two TMDs are also predicted in the malaria parasite *Plasmodium falciparum* (Ayong *et al.*, 2007), although the structural topology and functions of these proteins remain elusive. Molecular and functional analyses of these uniquely acquired SNARE proteins to each lineage, including Myr-VAMP72, will provide deeper insights into the diversification and evolution of membrane trafficking pathways that are associated with the diversification and/or acquisition of SNARE molecules during the evolution of eukaryotic cells.

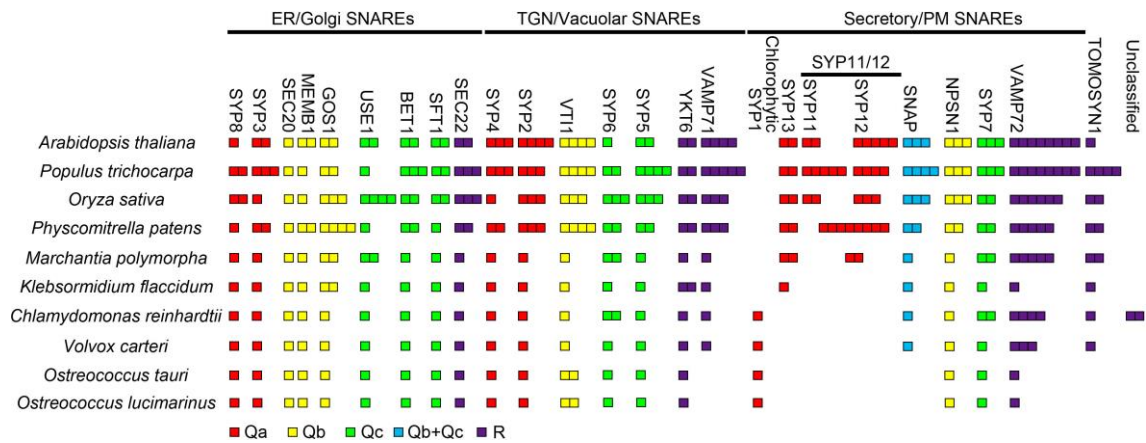


Figure 3-1. SNARE genes in green plants

SNAREs are classified into three major categories: ER/Golgi SNAREs, TGN/Vacuolar SNAREs, and Secretory/PM SNAREs, according to Sanderfoot (2007). The names given to the plant orthologs are shown below the classification. SNARE genes are indicated as individual boxes regardless of the presence of splicing variants, and each class of SNARE proteins is indicated in a different color (Qa, red; Qb, yellow; Qc, green, Qb+Qc, cyan; R, purple). The accession numbers of the SNARE genes for the listed organisms excluding *M. polymorpha* and *K. flaccidum* were retrieved from Sanderfoot 2007.

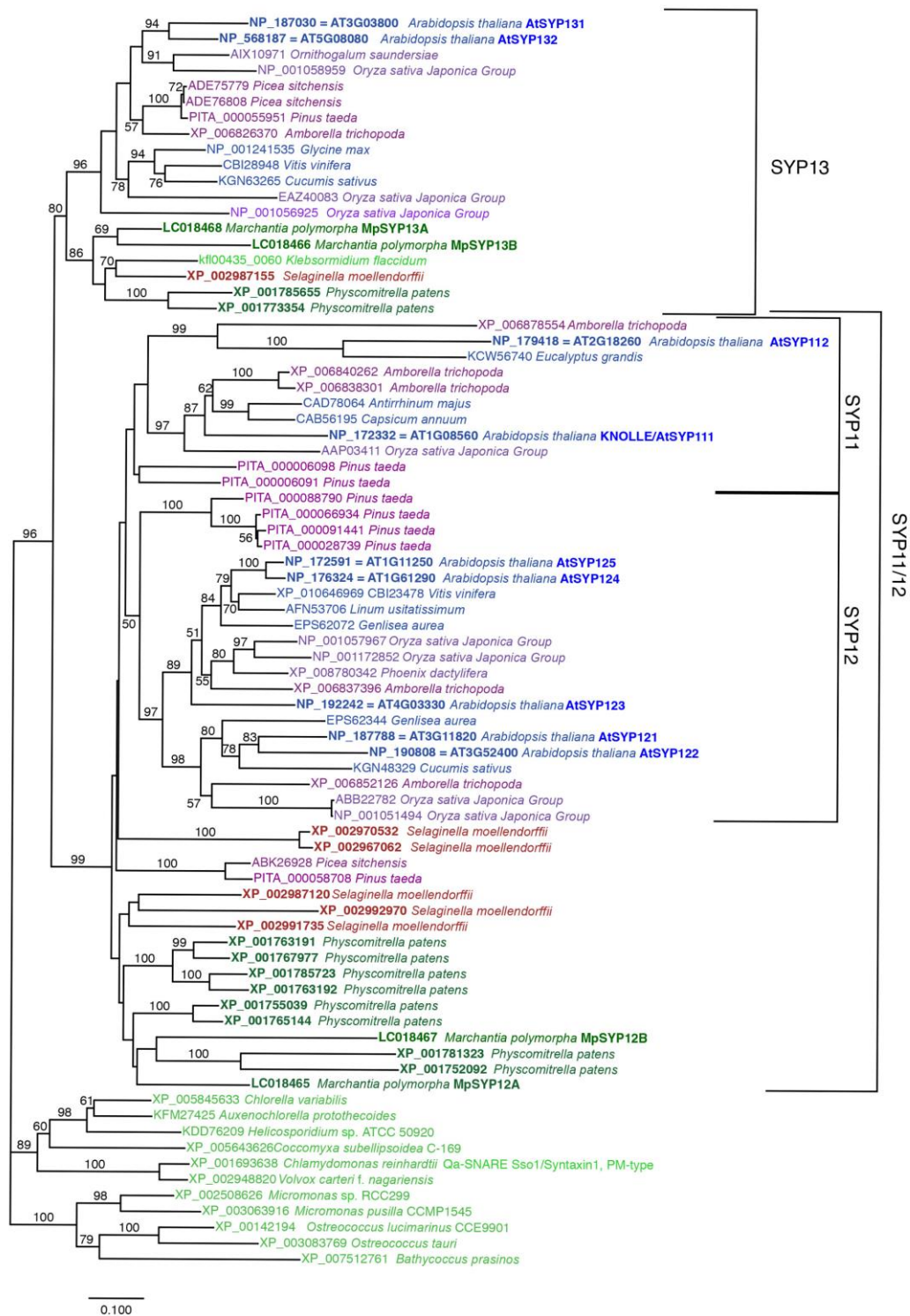


Figure 3-2. Neighbor Joining tree of the green plant SYP1 group

Amino acid substitution model of JTT (1992) was used. The tree is unrooted but drawn with proteins of chlorophytes as the outgroup to proteins of streptophytes. The branch lengths are proportional to the estimated number of substitution per site.

Figure 3-2. (continued)

Bootstrap probability is indicated as percentage on each branch with at least 50% support. Sequences from the NCBI database are labeled by their accession numbers. Organism names are given next to the accession number. For *A. thaliana* genes, the AGI codes and short names are given. Sequences from other sources have their own identifiers. The color of the label is according to the classification, blue: eudicots, blue violet: monocots, dark magenta: basal angiosperms (Amborella) and gymnosperms, brown: lycophytes (Selaginella), green: bryophytes, light green: green algae.



Figure 3-3. Sequence alignment of SYP1 proteins of *M. polymorpha*

Amino acid sequences of four MpSYP1 members are aligned. The syntaxin domain (red line), SNARE domain (purple line), and transmembrane domain (TMD, light blue line) are indicated above the sequences. Identical (asterisk), highly-conserved (colon), and weakly-conserved (period) amino acid residues are indicated.

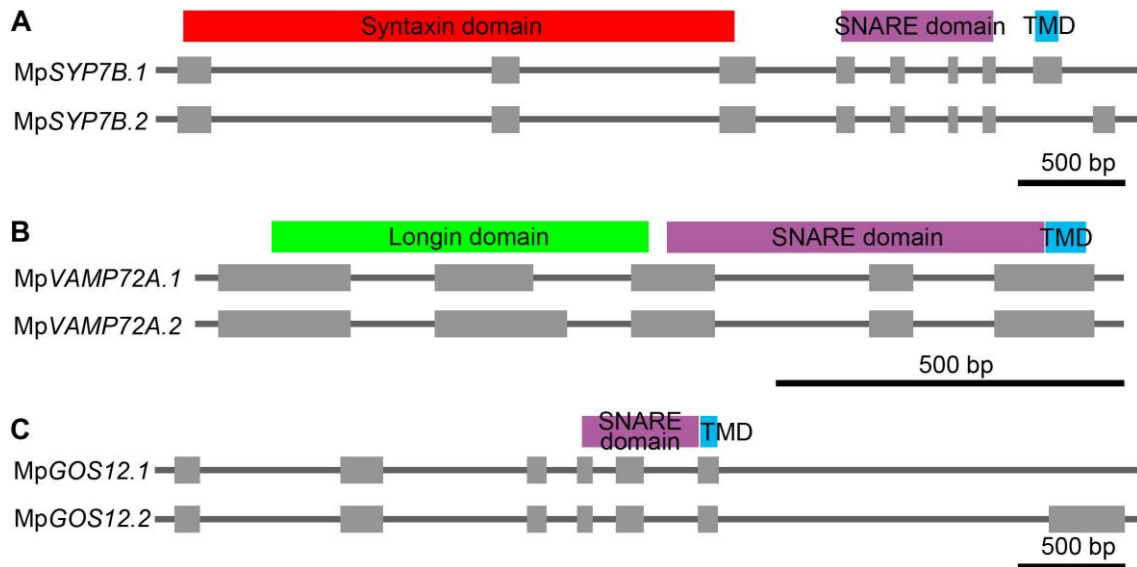


Figure 3-4. Schematic models of SNARE genes with splicing variants

(A) Two transcripts derived from the *MpSYP7B* locus; one harbors a TMD, whereas the other lacks a TMD. (B) Two transcripts derived from the *MpVAMP72A* locus; the lengths of the longin domain vary between the two products. (C) Two transcripts derived from the *MpGOS12* locus; the lengths of the carboxyl termini vary between the two products. Gray boxes indicate protein-coding regions. Black bars = 500 bp.

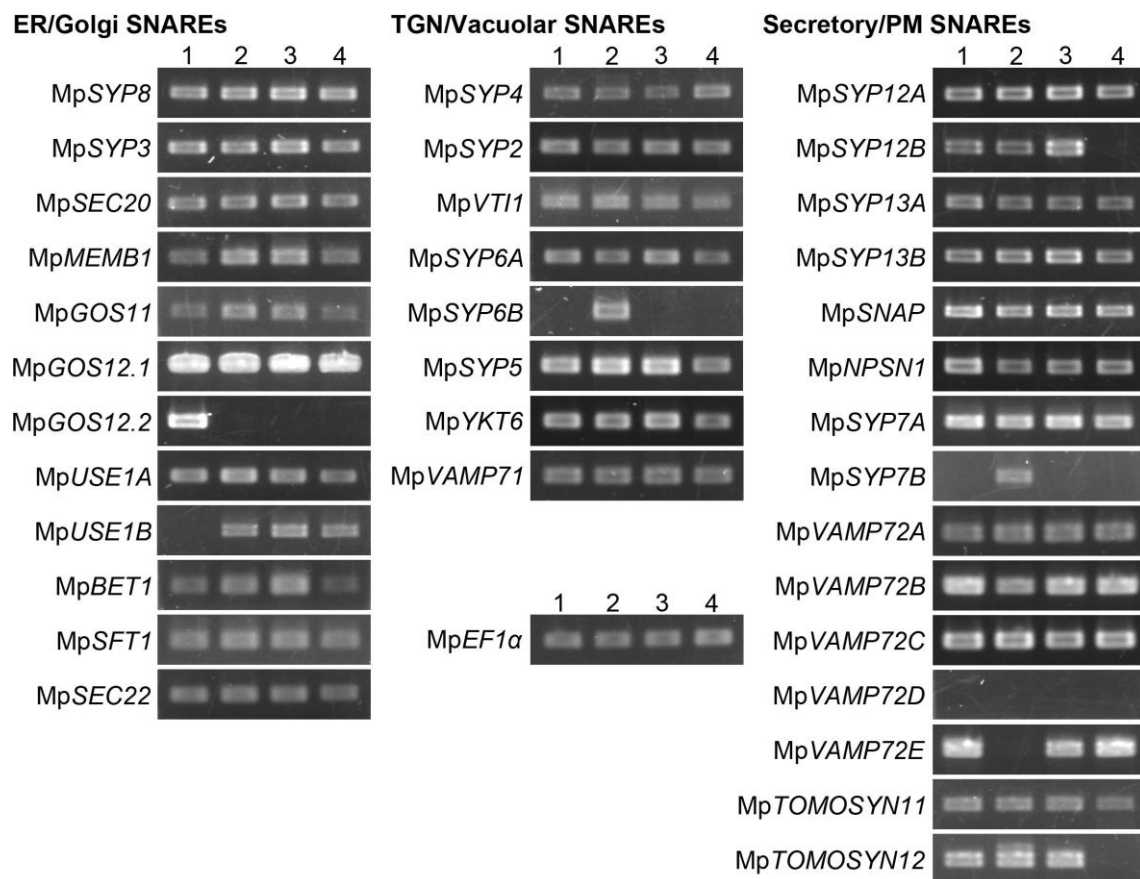


Figure 3-5. Transcription of SNARE genes in *M. polymorpha*

Total RNA samples were extracted from 5-day-old thalli (lane 1), antheridiophores (lane 2), archegoniophores (lane 3), and 7-day-old sporelings (lane 4), which were subjected to RT-PCR. The amounts of template cDNA were adjusted based on the MpEF1α expression.

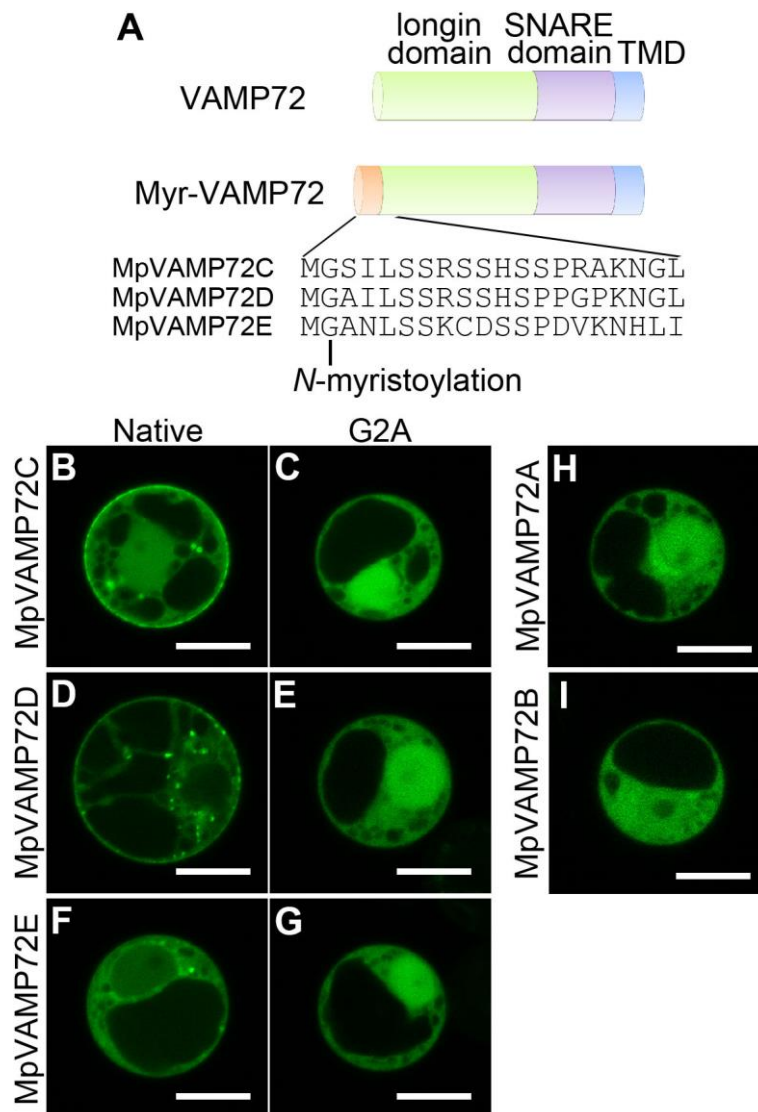


Figure 3-6. *M. polymorpha* harbors unique VAMP72 members

(A) Schematic primary structures of VAMP72 proteins in *M. polymorpha*. Canonical VAMP72 consists of the longin domain, SNARE domain, and transmembrane domain (TMD). In addition to these three domains, *N*-myristoylated VAMP72 (Myr-VAMP72) extends at the amino terminus, which contains the consensus for *N*-myristoylation. (B–I) Confocal images of protoplasts of *A. thaliana* cells cultured in suspension expressing YFP fused with the twenty N-terminal amino acid residues of the MpVAMP72 members. The N-terminal sequences of Myr-VAMP72 [MpVAMP72C (B), MpVAMP72D (D), and MpVAMP72E (F)] deliver YFP to the endomembrane compartments, although the N-terminal sequences of canonical VAMP72 [MpVAMP72A (H) and MpVAMP72B (I)] and mutated sequences of Myr-VAMP72 (G2A) [MpVAMP72C (C), MpVAMP72D (E), and MpVAMP72E (G)] do not. Scale bars = 10 μ m.

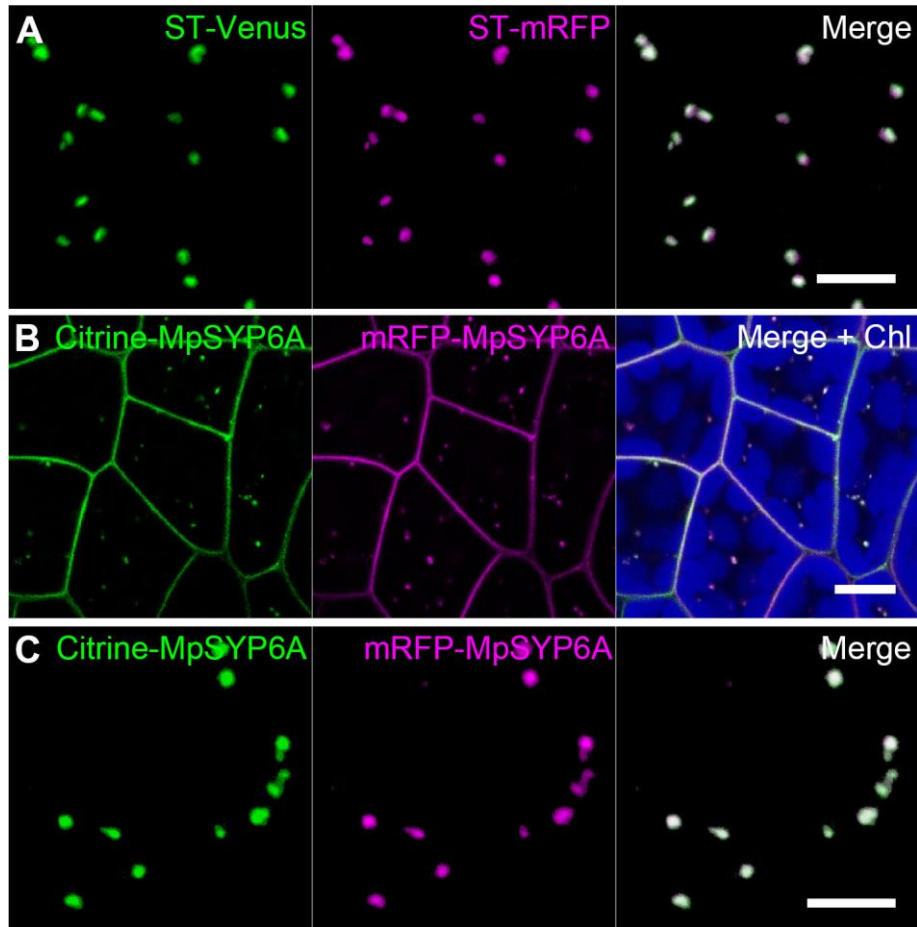


Figure 3-7. Markers of the Golgi apparatus and *trans*-Golgi network (TGN) in *M. polymorpha*

(A) Maximum intensity projection images of *M. polymorpha* thallus cells expressing ST-Venus and ST-mRFP. (B) Single confocal images of *M. polymorpha* thallus cells expressing Citrine-MpSYP6A and mRFP-MpSYP6A. (C) Maximum intensity projection images of *M. polymorpha* thallus cells expressing Citrine-MpSYP6A and mRFP-MpSYP6A.

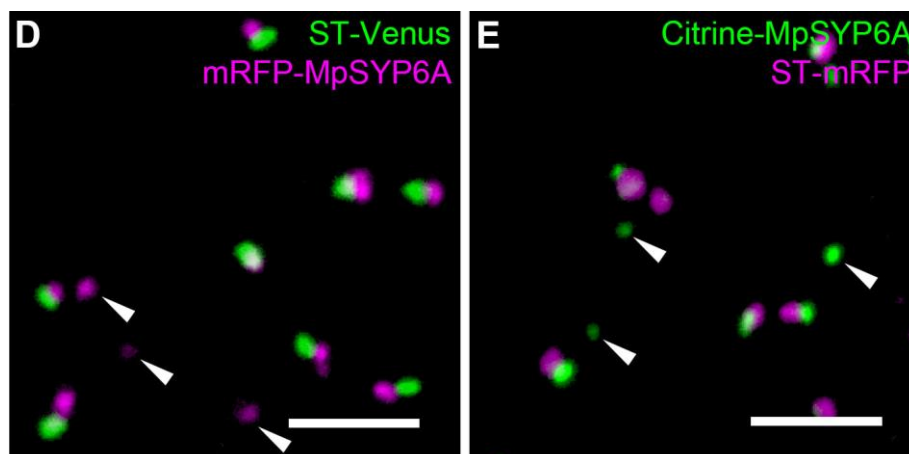


Figure 3-7. (continued)

(D) Maximum intensity projection images of *M. polymorpha* thallus cells expressing ST-Venus and mRFP-MpSYP6A. White arrowheads indicate the Golgi-independent TGN. (E) Maximum intensity projection images of *M. polymorpha* thallus cells expressing Citrine-MpSYP6A and ST-mRFP. White arrowheads indicate the Golgi-independent TGN. Green, magenta, and blue pseudo colors indicate fluorescence from YFP (Citrine or Venus), mRFP, and chlorophyll, respectively. Scale bars = 5 μm in (A), (C), (D), and (E), 10 μm in (B).

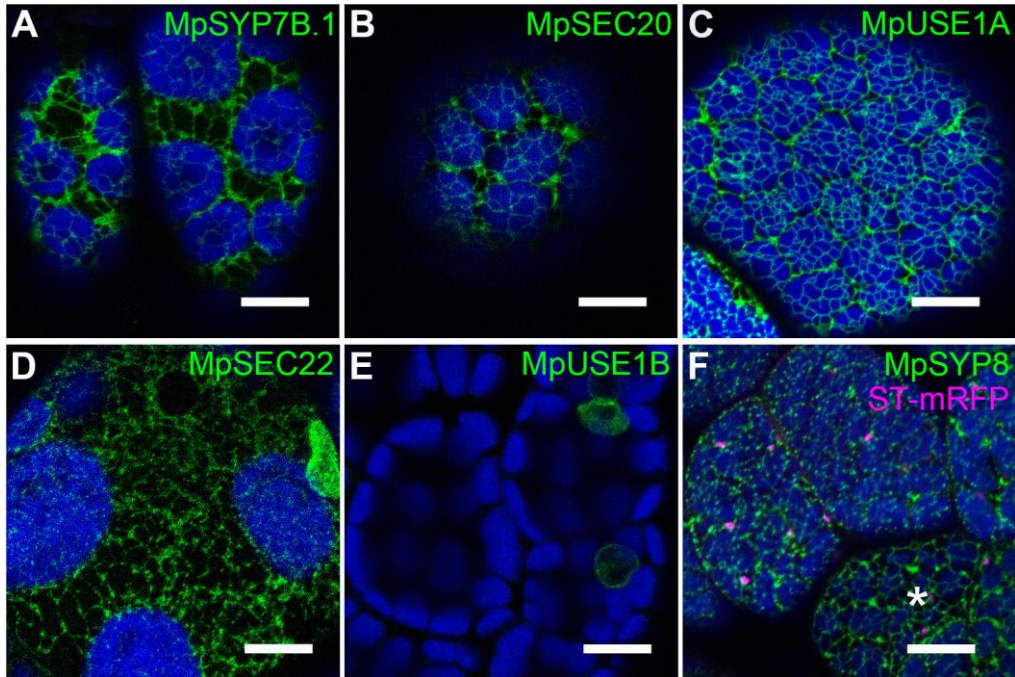


Figure 3-8. SNAREs localized to the ER

Single confocal images of *M. polymorpha* thallus cells expressing Citrine-MpSYP7B.1 (A), Citrine-MpSEC20 (B), Citrine-MpUSE1A (C), Citrine-MpSEC22 (D), Citrine-MpUSE1B (E), or Citrine-MpSYP8 and ST-mRFP (F). Green, magenta, and blue pseudo colors indicate fluorescence from Citrine, mRFP, and chlorophyll, respectively. Scale bars = 10 μm .

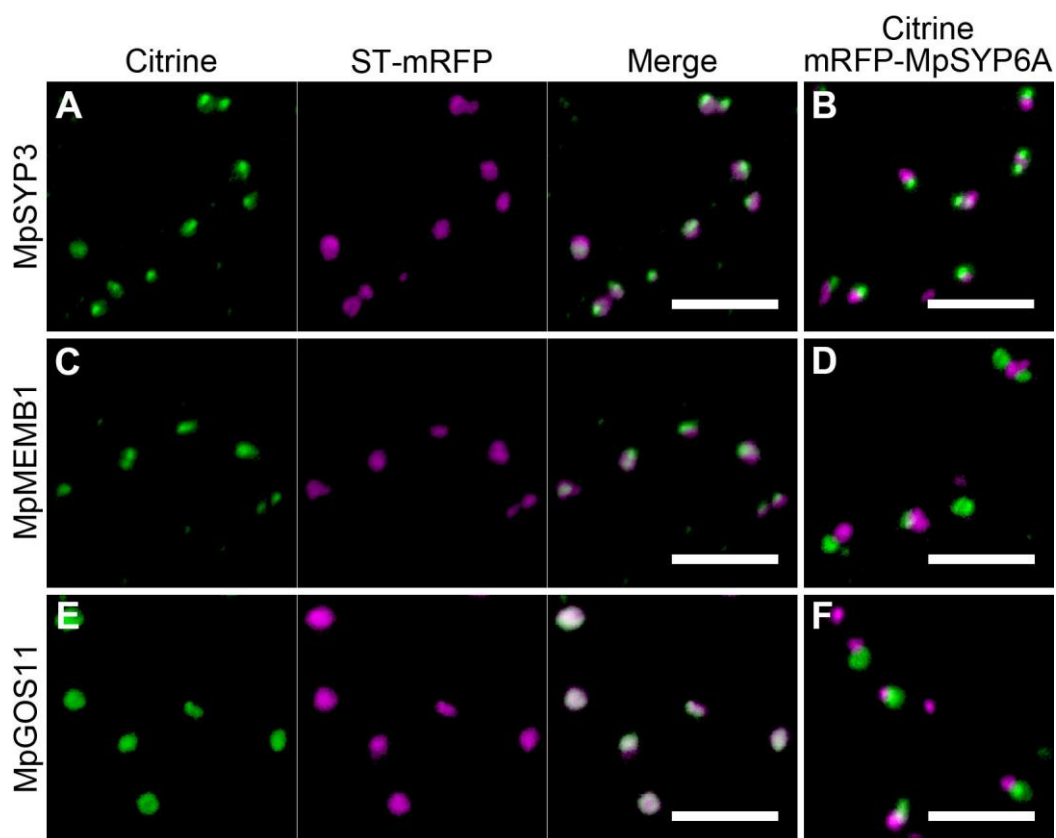


Figure 3-9. Golgi apparatus-localized SNAREs

Colocalization of Golgi-localized SNAREs with the marker for the Golgi apparatus (ST-mRFP) or the TGN (mRFP-MpSYP6A). (A, C, E, G, I, K, and M) Maximum intensity projection images of *M. polymorpha* thallus cells expressing ST-mRFP and Citrine-MpSYP3 (A), Citrine-MpMEMB1 (C), Citrine-MpGOS11 (E), Citrine-MpGOS12.1 (G), Citrine-MpGOS12.2 (I), Citrine-MpSFT1 (K), or Citrine-MpTOMOSYN11 (M). (B, D, F, H, J, L, and N) Maximum intensity projection images of *M. polymorpha* thallus cells expressing mRFP-MpSYP6A and Citrine-MpSYP3 (B), Citrine-MpMEMB1 (D), Citrine-MpGOS11 (F), Citrine-MpGOS12.1 (H), Citrine-MpGOS12.2 (J), Citrine-MpSFT1 (L), or Citrine-MpTOMOSYN11 (N). The green and magenta pseudo colors indicate fluorescence from Citrine and mRFP, respectively. Scale bars = 5 μ m.

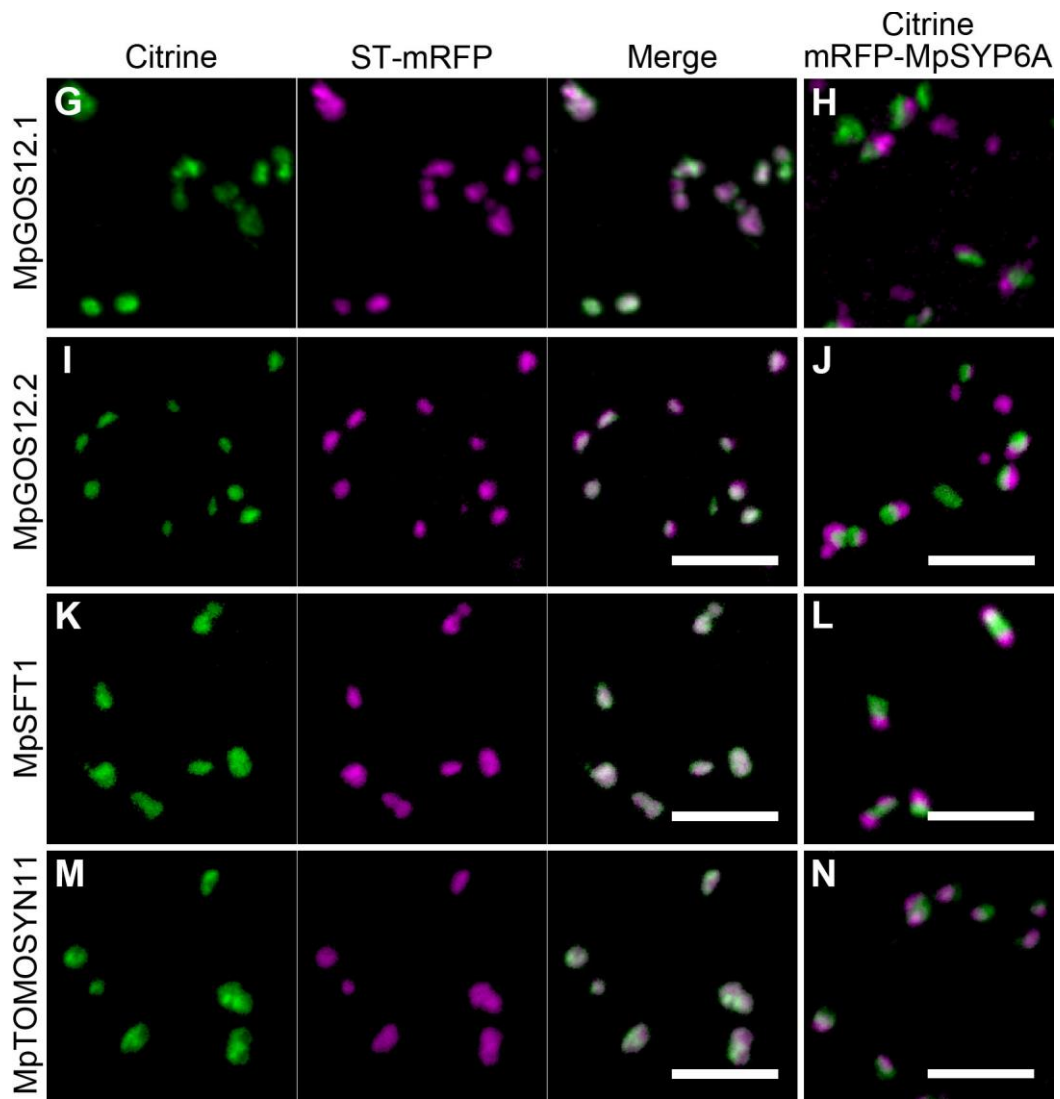


Figure 3-9. (continued)

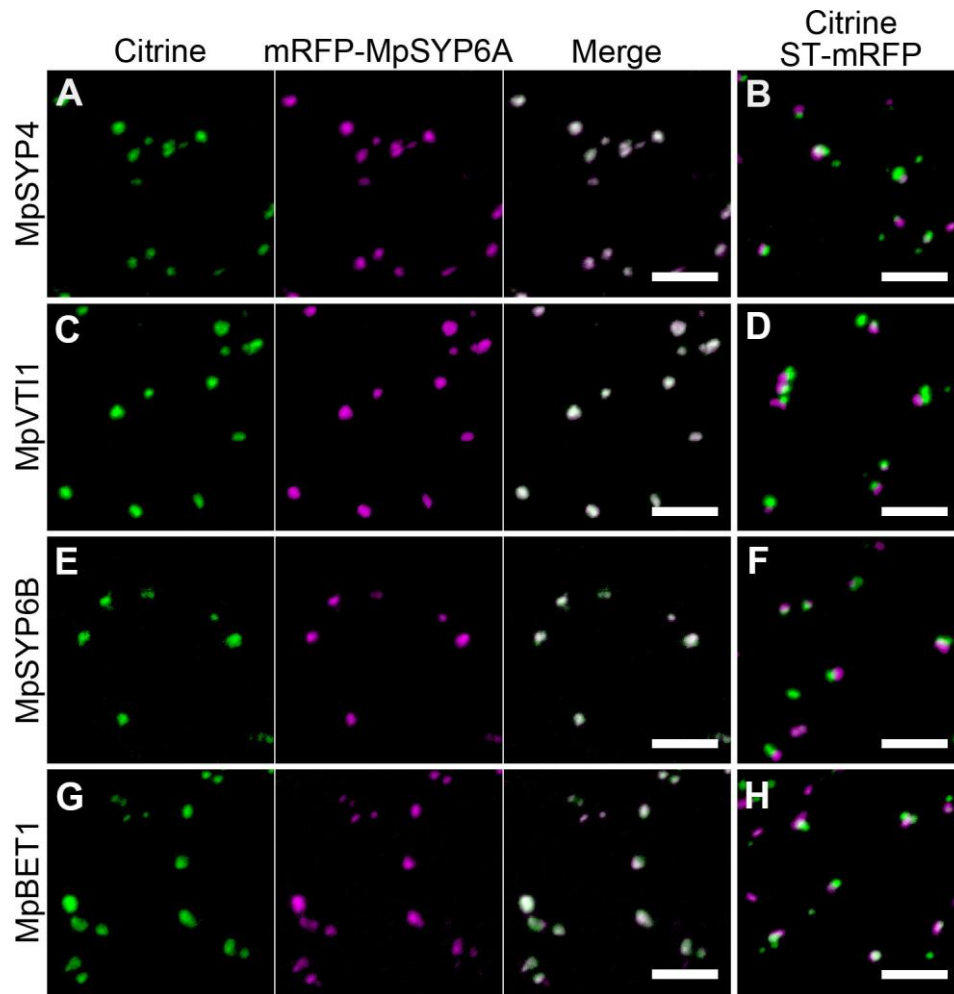


Figure 3-10. TGN-localized SNAREs

Colocalization of TGN-localized SNAREs with the marker for the TGN (mRFP-MpSYP6A) or the Golgi apparatus (ST-mRFP). (A, C, E, G) Maximum intensity projection images of *M. polymorpha* thallus cells expressing mRFP-MpSYP6A and Citrine-MpSYP4 (A), Citrine-MpVTI1 (C), Citrine-MpSYP6B (E), or Citrine-MpBET1 (G). (B, D, F, H) Maximum intensity projection images of *M. polymorpha* thallus cells expressing ST-mRFP and Citrine-MpSYP4 (B), Citrine-MpVTI1 (D), Citrine-MpSYP6B (F), or Citrine-MpBET1 (H). The green and magenta pseudo colors indicate fluorescence from Citrine and mRFP, respectively. Scale bars = 5 μ m.

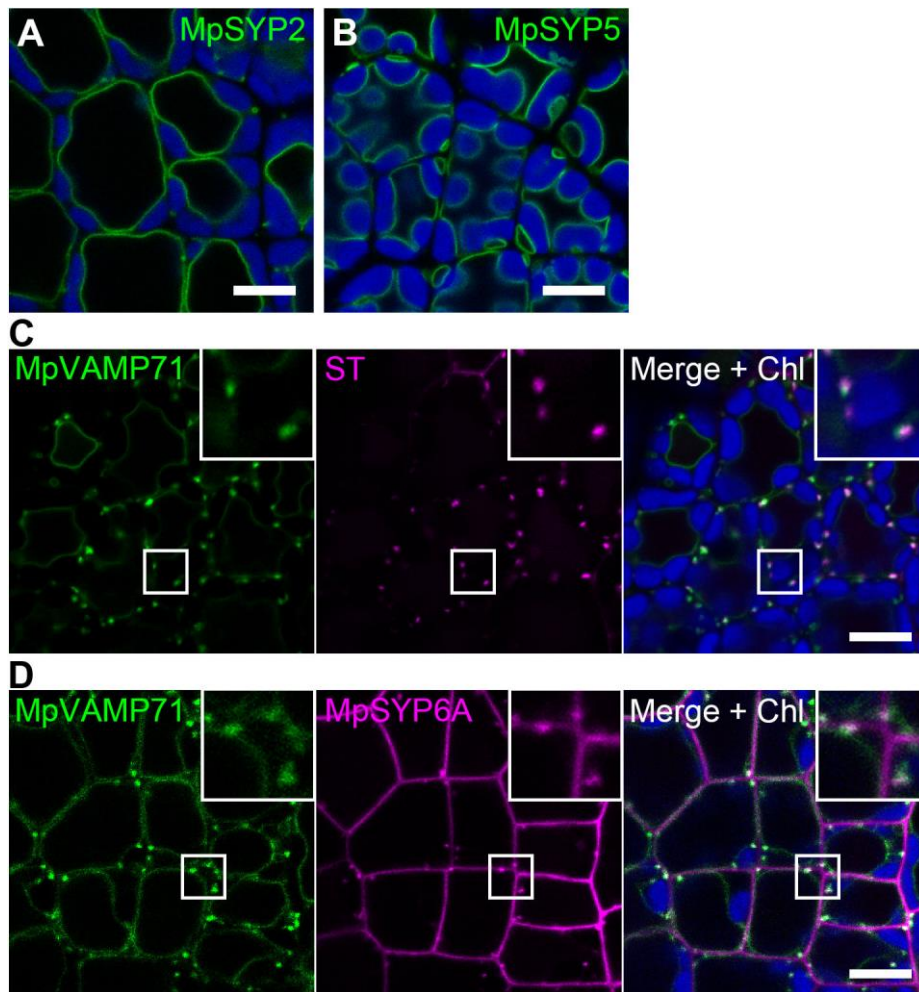


Figure 3-11. Vacuolar membrane-localized SNAREs

(A and B) Single confocal images of *M. polymorpha* thallus cells expressing Citrine-MpSYP2 (A) or Citrine-MpSYP5 (B) under the regulation of the CaMV 35S promoter. (C and D) Single confocal images of *M. polymorpha* thallus cells expressing Citrine-MpVAMP71 and ST-mRFP (C) or mRFP-MpSYP6A (D). The insets are magnified images of the boxed regions in (C) and (D). Green, magenta, and blue pseudo colors indicate fluorescence from Citrine, mRFP, and chlorophyll, respectively. Scale bars = 10 μm .

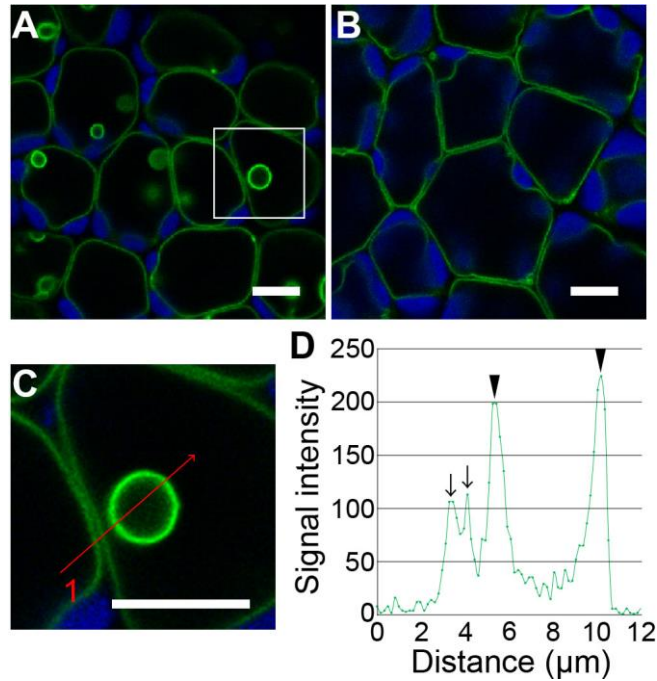


Figure 3-12. Potential effect of dimerization and overexpression on the localization of fluorescently tagged MpSYP2

(A) A single confocal image of *M. polymorpha* thallus cells expressing MpSYP2 tagged with Citrine under the regulation of the CaMV 35S promoter. (B) A single confocal image of *M. polymorpha* thallus cells expressing MpSYP2 tagged with mCitrine under the regulation of the MpSYP2 promoter. (C) Magnified image of the boxed region in B. (D) Fluorescence intensity of Citrine along the red arrow (1) in (C). Arrows indicate vacuolar membranes, and arrowheads indicate the membrane of the bulb. Scale bars = 10 μm .

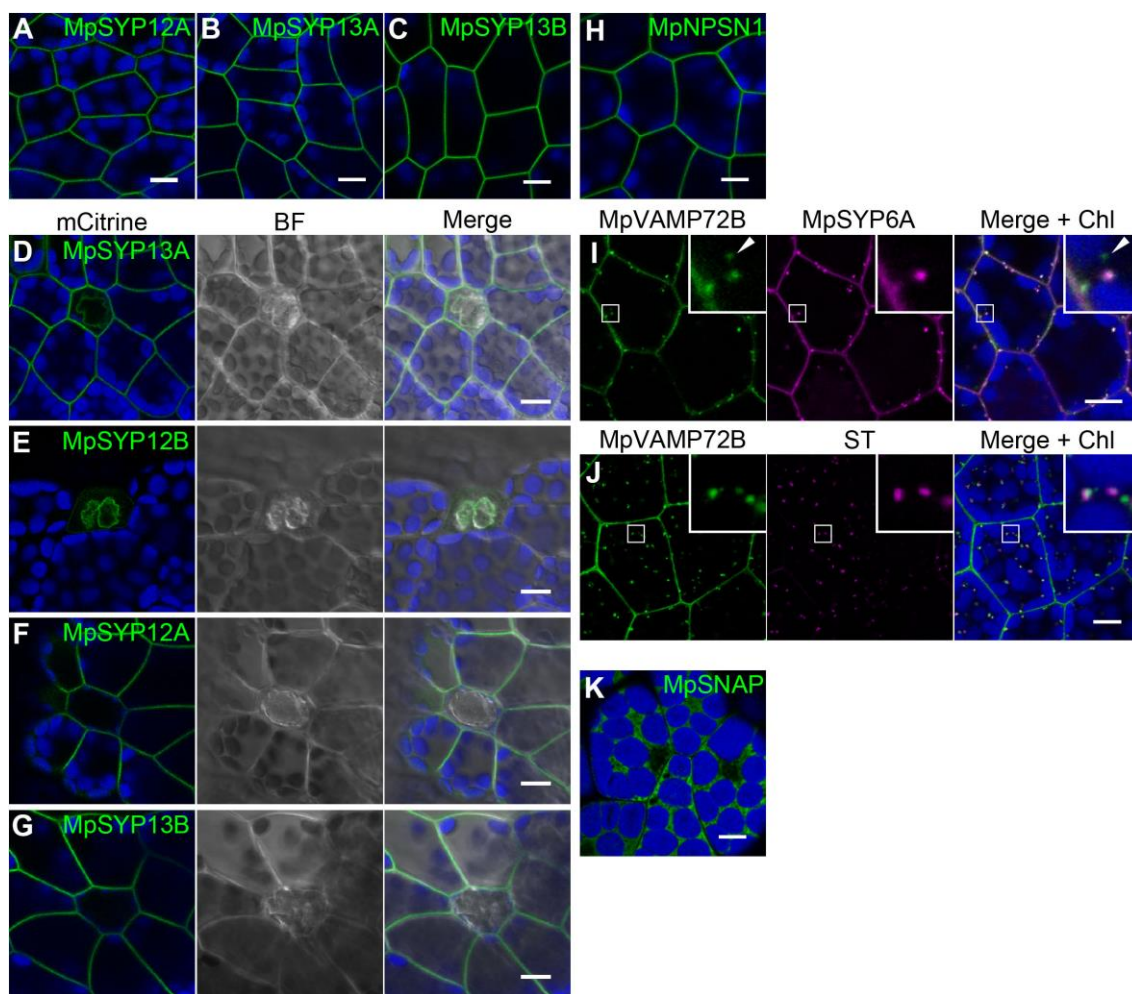


Figure 3-13 PM- and oil body membrane-localized SNAREs

(A–C) Single confocal images of *M. polymorpha* thallus cells expressing mCitrine-MpSYP12A (A), mCitrine-MpSYP13A (B), or mCitrine-MpSYP13B (C) under the regulation of their own promoters. (D–G) Single confocal images of *M. polymorpha* thallus cells expressing mCitrine-MpSYP13A (D), mCitrine-MpSYP12B (E), mCitrine-MpSYP12A (F), or MpSYP13B (G) driven by their own promoters. BF, bright field images. (H) A single confocal image of *M. polymorpha* thallus cells expressing Citrine-MpNPSN1 under the regulation of the CaMV 35S promoter. (I and J) Single confocal images of *M. polymorpha* thallus cells expressing Citrine-MpVAMP72B and mRFP-MpSYP6A (I), or Citrine-MpVAMP72B and ST-mRFP, under the regulation of the CaMV 35S promoter (J). The insets are magnified images of the boxed regions in (I) and (J). (K) A single confocal image of *M. polymorpha* thallus cells expressing Citrine-MpSNAP under the regulation of the CaMV 35S promoter. Green, magenta, and blue pseudo colors indicate fluorescence from (m)Citrine, mRFP, and chlorophyll, respectively. Scale bars = 10 μm .

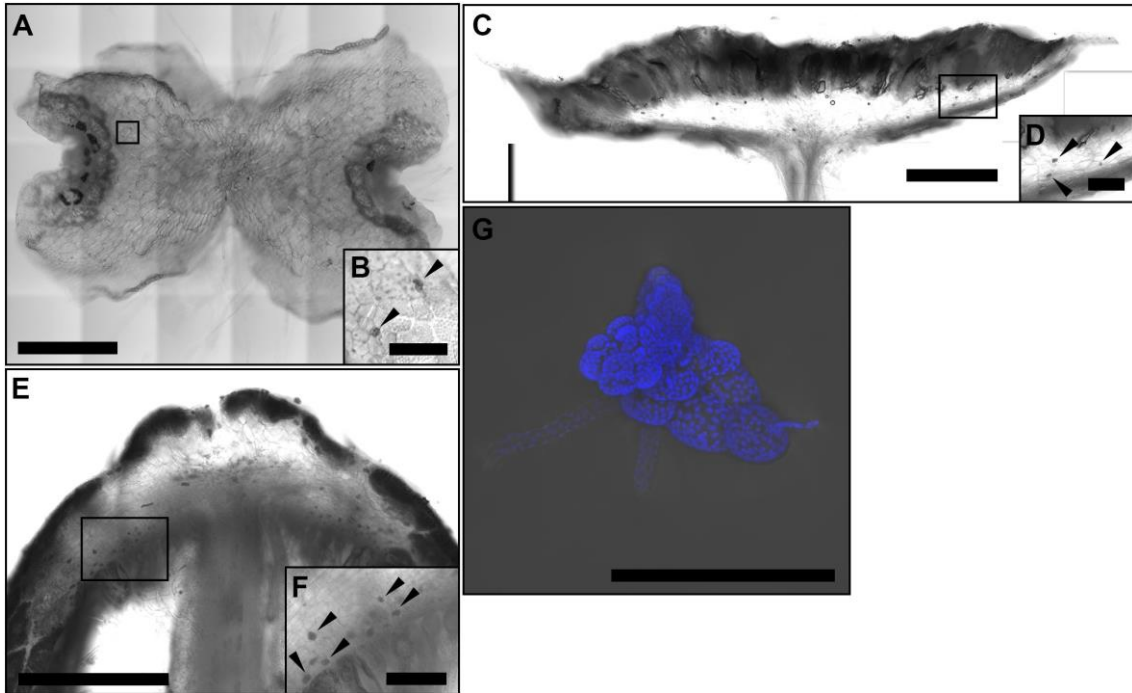


Figure 3-14 Distribution of oil body cells in *M. polymorpha*

(A–F) Bright field (BF) images of a 5-day-old thallus (A and B), an antheridiophore (C and D), and an archegoniophore (E and F). Magnified images of the boxed regions in (A), (C), and (E) are presented as (B), (D), and (F), respectively. Arrowheads indicate oil bodies. (G) A maximum intensity projection image of a 7-day-old sporeling overlaid on the BF image. The blue pseudo color indicates autofluorescence from chlorophyll. Scale bars = 1 mm in (A), (C), and (E), 100 μm in (B), and 200 μm in (D), (F), and (G).

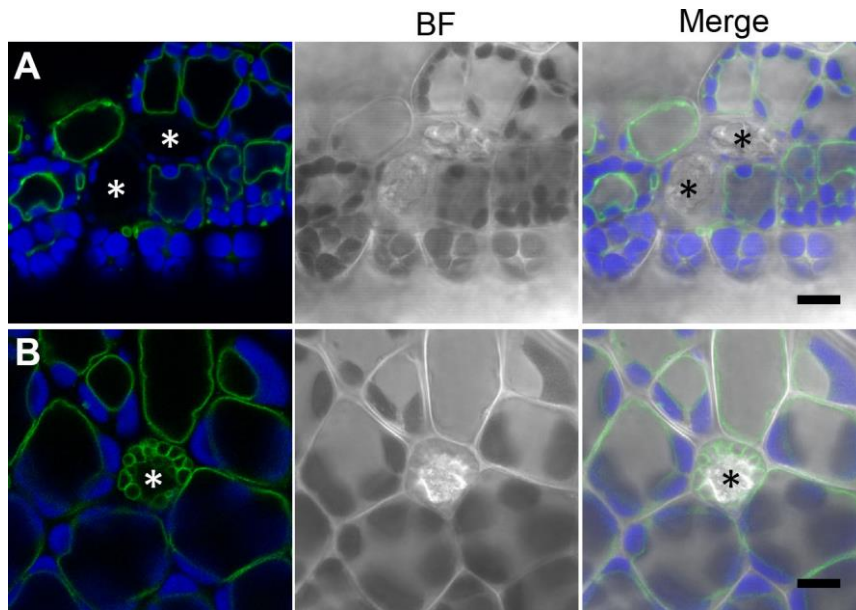


Figure 3-15 Inactivation of the CaMV 35S promoter in oil body cells.

(A) Single confocal images of *M. polymorpha* thallus cells expressing Citrine-MpSYP2 under the regulation of the CaMV 35S promoter. The Citrine signal is not visible in oil body cells (asterisks). (B) Single confocal images of *M. polymorpha* thallus cells expressing mCitrine-MpSYP2 under the regulation of the MpSYP2 promoter. The vacuolar membrane in an oil body cell (asterisk) is visualized using mCitrine. Scale bars = 10 μm .

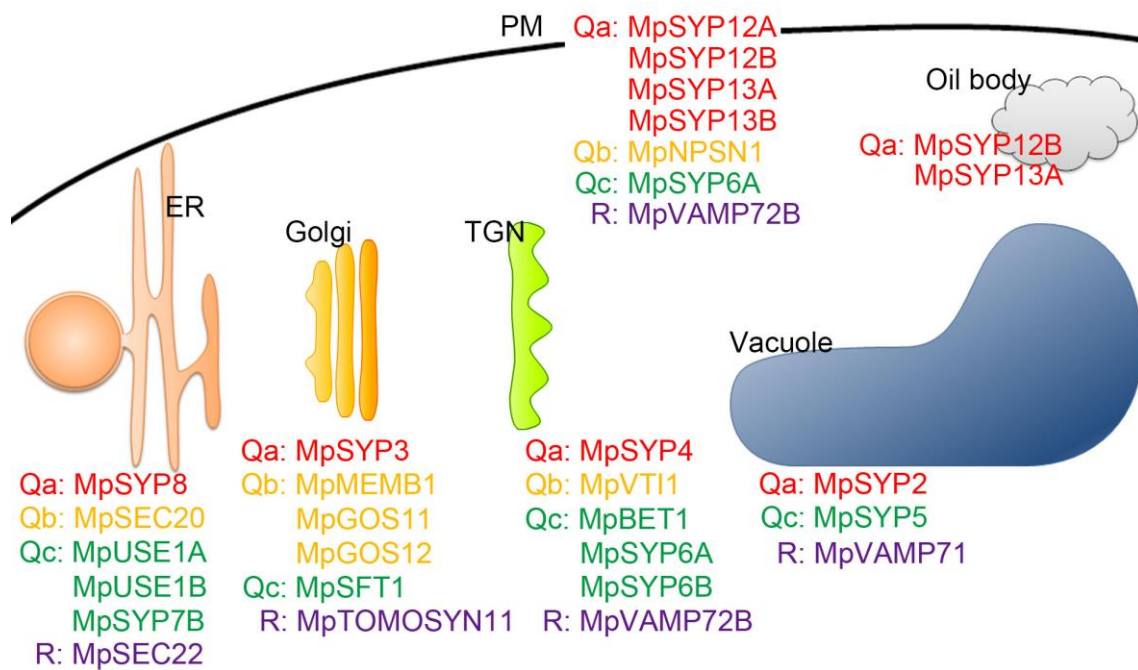


Figure 3-16 Schematic representation of the SNARE distribution in *M. polymorpha*
Subcellular localization of SNARE proteins determined under my experimental conditions.

Chapter IV: Cell-specific redirection of the secretory trafficking pathway lead to acquisition of new organelles during land plant evolution

第4章

本章については、5年以内に雑誌等で刊行予定のため、非公開。

Chapter V: Screening for mutants of oil body biogenesis and morphogenesis

第5章

本章については、5年以内に雑誌等で刊行予定のため、非公開。

Chapter VI: **Conclusion**

第 6 章

本章については、5年以内に雑誌等で刊行予定のため、非公開。

The main part of Chapter II and III has been published on *Plant and Cell Physiology* (Oxford University Press) as an article entitled “SNARE Molecules in *Marchantia polymorpha*: Unique and Conserved Features of the Membrane Fusion Machinery.” by T. Kanazawa, A. Era, N. Minamino, Y. Shikano, M. Fujimoto, T. Uemura, R. Nishihama, K.T. Yamato, K. Ishizaki, T. Nishiyama, T. Kohchi, A. Nakano, and T. Ueda (2016, volume 57, Issue 2, pages 307-324).

References

- Abbal P, Pradal M, Muniz L, Sauvage FX, Chatelet P, Ueda T, Tesniere C. 2008.** Molecular characterization and expression analysis of the Rab GTPase family in *Vitis vinifera* reveal the specific expression of a VvRabA protein. *J Exp Bot* **59**(9): 2403-2416.
- Althoff F, Kopischke S, Zobell O, Ide K, Ishizaki K, Kohchi T, Zachgo S. 2013.** Comparison of the MpEF1alpha and CaMV35 promoters for application in *Marchantia polymorpha* overexpression studies. *Transgenic Res* **23**(2): 235-244.
- Antonin W, Fasshauer D, Becker S, Jahn R, Schneider TR. 2002.** Crystal structure of the endosomal SNARE complex reveals common structural principles of all SNAREs. *Nat Struct Biol* **9**(2): 107-111.
- Arabidopsis Genome I. 2000.** Analysis of the genome sequence of the flowering plant *Arabidopsis thaliana*. *Nature* **408**(6814): 796-815.
- Asakawa Y. 2012.** Liverworts-potential source of medicinal compounds. *Pharm Biol* **50**(5): 662-662.
- Asakawa Y, Ludwiczuk A, Nagashima F. 2013.** Phytochemical and biological studies of bryophytes. *Phytochemistry* **91**: 52-80.
- Asakawa YT, M. Matsuda, K. Takikawa, K. Takemoto, T. 1983.** Distribution of novel cyclic bisbibenzyls in *Marchantia* and *Riccardia* species. *Phytochemistry* **22**(6): 3.
- Asaoka R, Uemura T, Ito J, Fujimoto M, Ito E, Ueda T, Nakano A. 2012.** Arabidopsis RABA1 GTPases are involved in transport between the *trans*-Golgi network and the plasma membrane, and are required for salinity stress tolerance. *Plant J* **73**(2): 240-249.
- Assaad FF, Qiu JL, Youngs H, Ehrhardt D, Zimmerli L, Kalde M, Wanner G, Peck SC, Edwards H, Ramonell K, Somerville CR, Thordal-Christensen H. 2004.** The PEN1 syntaxin defines a novel cellular compartment upon fungal attack and is required for the timely assembly of papillae. *Mol Biol Cell* **15**(11): 5118-5129.
- Ayong L, Pagnotti G, Tobon AB, Chakrabarti D. 2007.** Identification of *Plasmodium falciparum* family of SNAREs. *Mol Biochem Parasitol* **152**(2): 113-122.
- Banfield DK, Lewis MJ, Pelham HR. 1995.** A SNARE-like protein required for traffic through the Golgi complex. *Nature* **375**(6534): 806-809.
- Banks JA, Nishiyama T, Hasebe M, Bowman JL, Gribskov M, dePamphilis C, Albert VA, Aono N, Aoyama T, Ambrose BA, Ashton NW, Axtell MJ, Barker**

- E, Barker MS, Bennetzen JL, Bonawitz ND, Chapple C, Cheng C, Correa LG, Dacre M, DeBarry J, Dreyer I, Elias M, Engstrom EM, Estelle M, Feng L, Finet C, Floyd SK, Frommer WB, Fujita T, Gramzow L, Gutensohn M, Harholt J, Hattori M, Heyl A, Hirai T, Hiwatashi Y, Ishikawa M, Iwata M, Karol KG, Koehler B, Kolukisaoglu U, Kubo M, Kurata T, Lalonde S, Li K, Li Y, Litt A, Lyons E, Manning G, Maruyama T, Michael TP, Mikami K, Miyazaki S, Morinaga S, Murata T, Mueller-Roeber B, Nelson DR, Obara M, Oguri Y, Olmstead RG, Onodera N, Petersen BL, Pils B, Prigge M, Rensing SA, Riano-Pachon DM, Roberts AW, Sato Y, Scheller HV, Schulz B, Schulz C, Shakhov I, Shibagaki N, Shinohara N, Shippen DE, Sorensen I, Sotooka R, Sugimoto N, Sugita M, Sumikawa N, Tanurdzic M, Theissen G, Ulvskov P, Wakazuki S, Weng JK, Willats WW, Wipf D, Wolf PG, Yang L, Zimmer AD, Zhu Q, Mitros T, Hellsten U, Loque D, O'tillar R, Salamov A, Schmutz J, Shapiro H, Lindquist E, Lucas S, Rokhsar D, Grigoriev IV. 2011. The *Selaginella* genome identifies genetic changes associated with the evolution of vascular plants. *Science* 332(6032): 960-963.
- Barker MS, Vogel H, Schranz ME. 2009.** Paleopolyploidy in the Brassicales: analyses of the *Cleome* transcriptome elucidate the history of genome duplications in *Arabidopsis* and other Brassicales. *Genome Biol Evol* 1: 391-399.
- Barr FA, Gruneberg U. 2007.** Cytokinesis: placing and making the final cut. *Cell* 131(5): 847-860.
- Bassham DC, Gal S, da Silva Conceicao A, Raikhel NV. 1995.** An *Arabidopsis* syntaxin homologue isolated by functional complementation of a yeast *pep12* mutant. *Proc Natl Acad Sci U S A* 92(16): 7262-7266.
- Bassham DC, Sanderfoot AA, Kovaleva V, Zheng H, Raikhel NV. 2000.** AtVPS45 complex formation at the *trans*-Golgi network. *Mol Biol Cell* 11(7): 2251-2265.
- Bergdolt E. 1926.** Untersuchungen über Marchantiaceen. *Bot. Abh.* 10: 1-86.
- Bock JB, Matern HT, Peden AA, Scheller RH. 2001.** A genomic perspective on membrane compartment organization. *Nature* 409(6822): 839-841.
- Boevink P, Oparka K, Santa Cruz S, Martin B, Betteridge A, Hawes C. 1998.** Stacks on tracks: the plant Golgi apparatus traffics on an actin/ER network. *Plant J* 15(3): 441-447.
- Bologna G, Yvon C, Duvaud S, Veuthey AL. 2004.** N-terminal myristoylation predictions by ensembles of neural networks. *Proteomics* 4(6): 1626-1632.
- Bolte S, Talbot C, Boutte Y, Catrice O, Read ND, Satiat-Jeunemaitre B. 2004.** FM-dyes as experimental probes for dissecting vesicle trafficking in living plant cells.

J Microsc **214**: 159-173.

- Borgese N, Francolini M, Snapp E. 2006.** Endoplasmic reticulum architecture: structures in flux. *Curr Opin Cell Biol* **18**(4): 358-364.
- Boutté Y, Frescatada-Rosa M, Men S, Chow CM, Ebine K, Gustavsson A, Johansson L, Ueda T, Moore I, Jurgens G, Grebe M. 2010.** Endocytosis restricts Arabidopsis KNOLLE syntaxin to the cell division plane during late cytokinesis. *EMBO J* **29**(3): 546-558.
- Bubeck J, Scheuring D, Hummel E, Langhans M, Viotti C, Foresti O, Denecke J, Banfield DK, Robinson DG. 2008.** The syntaxins SYP31 and SYP81 control ER-Golgi trafficking in the plant secretory pathway. *Traffic* **9**(10): 1629-1652.
- Carbonnier ML, Gavaudan, P. 1960.** Le probleme de l'origine des éléoplastes de la cellule des Hépatiques. *C R Séances Soc Biol* **154**: 1597-1601.
- Carter C, Pan S, Zouhar J, Avila EL, Girke T, Raikhel NV. 2004.** The vegetative vacuole proteome of *Arabidopsis thaliana* reveals predicted and unexpected proteins. *Plant Cell* **16**(12): 3285-3303.
- Chapman RL, Borkhsenius O, Brown RC, Henk MC, Waters DA. 2001.** Phragmoplast-mediated cytokinesis in *Trentepohlia*: results of TEM and immunofluorescence cytochemistry. *Int J Syst Evol Microbiol* **51**(Pt 3): 759-765.
- Chatre L, Brandizzi F, Hocquellet A, Hawes C, Moreau P. 2005.** Sec22 and Memb11 are v-SNAREs of the anterograde endoplasmic reticulum-Golgi pathway in tobacco leaf epidermal cells. *Plant Physiol* **139**(3): 1244-1254.
- Chiyoda S, Ishizaki K, Kataoka H, Yamato KT, Kohchi T. 2008.** Direct transformation of the liverwort *Marchantia polymorpha* L. by particle bombardment using immature thalli developing from spores. *Plant Cell Rep* **27**(9): 1467-1473.
- Chiyoda S, Linley PJ, Yamato KT, Fukuzawa H, Yokota A, Kohchi T. 2007.** Simple and efficient plastid transformation system for the liverwort *Marchantia polymorpha* L. suspension-culture cells. *Transgenic Res* **16**(1): 41-49.
- Choi SW, Tamaki T, Ebine K, Uemura T, Ueda T, Nakano A. 2013.** RABA members act in distinct steps of subcellular trafficking of the FLAGELLIN SENSING2 receptor. *Plant Cell* **25**(3): 1174-1187.
- Collins NC, Thordal-Christensen H, Lipka V, Bau S, Kombrink E, Qiu JL, Huckelhoven R, Stein M, Freialdenhoven A, Somerville SC, Schulze-Lefert P. 2003.** SNARE-protein-mediated disease resistance at the plant cell wall. *Nature* **425**(6961): 973-977.
- Cook ME. 2004.** Cytokinesis in *Coleochaete orbicularis* (Charophyceae): an ancestral mechanism inherited by plants. *Am J Bot* **91**(3): 313-320.

- Crandall-Stotler BS, E.R.; Long, G.D. . 2009.** Phylogeny and classification of the Marchantiophyta. *Edinb J Bot* **66**: 155 - 198.
- Crowell EF, Bischoff V, Desprez T, Rolland A, Stierhof YD, Schumacher K, Gonneau M, Hofte H, Vernhettes S. 2009.** Pausing of Golgi bodies on microtubules regulates secretion of cellulose synthase complexes in *Arabidopsis*. *Plant Cell* **21**(4): 1141-1154.
- Cui Y, Zhao Q, Gao C, Ding Y, Zeng Y, Ueda T, Nakano A, Jiang L. 2014.** Activation of the Rab7 GTPase by the MON1-CCZ1 complex is essential for PVC-to-vacuole trafficking and plant growth in *Arabidopsis*. *Plant Cell* **26**(5): 2080-2097.
- Dacks JB, Field MC. 2007.** Evolution of the eukaryotic membrane-trafficking system: origin, tempo and mode. *J Cell Sci* **120**(Pt 17): 2977-2985.
- Dacks JB, Poon PP, Field MC. 2008.** Phylogeny of endocytic components yields insight into the process of nonendosymbiotic organelle evolution. *Proc Natl Acad Sci U S A* **105**(2): 588-593.
- Dettmer J, Hong-Hermesdorf A, Stierhof YD, Schumacher K. 2006.** Vacuolar H⁺-ATPase activity is required for endocytic and secretory trafficking in *Arabidopsis*. *Plant Cell* **18**(3): 715-730.
- Dhonukshe P, Aniento F, Hwang I, Robinson DG, Mravec J, Stierhof YD, Friml J. 2007.** Clathrin-mediated constitutive endocytosis of PIN auxin efflux carriers in *Arabidopsis*. *Curr Biol* **17**(6): 520-527.
- Dhonukshe P, Baluska F, Schlicht M, Hlavacka A, Samaj J, Friml J, Gadella TWJ. 2006.** Endocytosis of cell surface material mediates cell plate formation during plant cytokinesis. *Dev Cell* **10**(1): 137-150.
- Dilcher M, Veith B, Chidambaram S, Hartmann E, Schmitt HD, Fischer von Mollard G. 2003.** Use1p is a yeast SNARE protein required for retrograde traffic to the ER. *EMBO J* **22**(14): 3664-3674.
- Dombarry P. 1926.** Contribution a l'étude des corps oléiformes des Hépatiques des environs de Nancy. *Thèses présentées à la Faculté des Sciences de l'Univesité de Paris*.
- Duckett JGL, R. 1995.** The formation of catenate foliar gemmae and the origin of oil bodies in the liverwort *Odontoschisma denudatum* (Mart.) Dum. (Jungermanniales): a Light and Electron Microscope Study *Ann Bot* **76**(4): 15.
- Ebine K, Fujimoto M, Okatani Y, Nishiyama T, Goh T, Ito E, Dainobu T, Nishitani A, Uemura T, Sato MH, Thordal-Christensen H, Tsutsumi N, Nakano A, Ueda T. 2011.** A membrane trafficking pathway regulated by the plant-specific RAB GTPase ARA6. *Nat Cell Biol* **13**(7): 853-859.

- Ebine K, Inoue T, Ito J, Ito E, Uemura T, Goh T, Abe H, Sato K, Nakano A, Ueda T. 2014.** Plant vacuolar trafficking occurs through distinctly regulated pathways. *Curr Biol* **24**(12): 1375-1382.
- Ebine K, Okatani Y, Uemura T, Goh T, Shoda K, Niihama M, Morita MT, Spitzer C, Otegui MS, Nakano A, Ueda T. 2008.** A SNARE complex unique to seed plants is required for protein storage vacuole biogenesis and seed development of *Arabidopsis thaliana*. *Plant Cell* **20**(11): 3006-3021.
- Edgar RC. 2004.** MUSCLE: multiple sequence alignment with high accuracy and high throughput. *Nucleic Acids Res* **32**(5): 1792-1797.
- El Kasmi F, Krause C, Hiller U, Stierhof YD, Mayer U, Conner L, Kong L, Reichardt I, Sanderfoot AA, Jurgens G. 2013.** SNARE complexes of different composition jointly mediate membrane fusion in *Arabidopsis* cytokinesis. *Mol Biol Cell* **24**(10): 1593-1601.
- Elias M. 2008.** The guanine nucleotide exchange factors Sec2 and PRONE: candidate synapomorphies for the Opisthokonta and the Archaeplastida. *Mol Biol Evol* **25**(8): 1526-1529.
- Elias M, Brighthouse A, Gabernet-Castello C, Field MC, Dacks JB. 2012.** Sculpting the endomembrane system in deep time: high resolution phylogenetics of Rab GTPases. *J Cell Sci* **125**(Pt 10): 2500-2508.
- Enami K, Ichikawa M, Uemura T, Kutsuna N, Hasezawa S, Nakagawa T, Nakano A, Sato MH. 2009.** Differential expression control and polarized distribution of plasma membrane-resident SYP1 SNAREs in *Arabidopsis thaliana*. *Plant Cell Physiol* **50**(2): 280-289.
- Era A. 2013.** Studies of membrane trafficking system of the basal land plant, *Marchantia polymorpha*. *Doctral thesis*.
- Era A, Kutsuna N, Higaki T, Hasezawa S, Nakano A, Ueda T. 2013.** Microtubule stability affects the unique motility of F-actin in *Marchantia polymorpha*. *J Plant Res* **126**(1): 113-119.
- Era A, Tominaga M, Ebine K, Awai C, Saito C, Ishizaki K, Yamato KT, Kohchi T, Nakano A, Ueda T. 2009.** Application of Lifeact reveals F-actin dynamics in *Arabidopsis thaliana* and the liverwort, *Marchantia polymorpha*. *Plant and Cell Physiology* **50**(6): 1041-1048.
- Fabon G, Monforte L, Tomas-Las-Heras R, Nunez-Olivera E, Martinez-Abaigar J. 2012.** Dynamic response of UV-absorbing compounds, quantum yield and the xanthophyll cycle to diel changes in UV-B and photosynthetic radiations in an aquatic liverwort. *J Plant Physiol* **169**(1): 20-26.

- Fang Y, Zhu RL, Mishler BD. 2014.** Evolution of oleosin in land plants. *PLoS One* **9**(8): e103806.
- Fasshauer D, Sutton RB, Brunger AT, Jahn R. 1998.** Conserved structural features of the synaptic fusion complex: SNARE proteins reclassified as Q- and R-SNAREs. *Proc Natl Acad Sci U S A* **95**(26): 15781-15786.
- Felsenstein J 2013.** PHYLIP (Phylogeny Inference Package) version 3.695. Seattle.: Distributed by the author. Department of Genome Sciences, University of Washington.
- Fujimoto M, Ueda T. 2012.** Conserved and plant-unique mechanisms regulating plant post-Golgi traffic. *Front Plant Sci* **3**: 197.
- Fujiwara M, Uemura T, Ebine K, Nishimori Y, Ueda T, Nakano A, Sato MH, Fukao Y. 2014.** Interactomics of Qa-SNARE in *Arabidopsis thaliana*. *Plant Cell Physiol* **55**(4): 781-789.
- Galatis B, Apostolakos P, Katsaros C. 1978a.** Histochemical studies on oil-bodies of *Marchantia paleacea* Bert. *Protoplasma* **97**(1): 13-29.
- Galatis B, Apostolakos P, Katsaros C. 1978b.** Ultrastructural studies on oil bodies of *Marchantia paleacea* Bert. I. Early stages of oil-body cell-differentiation - origination of oil body. *Can J Bot* **56**(18): 2252-2267.
- Galatis B, Katsaros C, Apostolakos P. 1978c.** Ultrastructural studies on oil bodies of *Marchantia paleacea* Bert. II. Advanced stages of oil-body cell-differentiation - synthesis of lipophilic material. *Can J Bot* **56**(18): 2268-2285.
- Gamborg OL, Miller RA, Ojima K. 1968.** Nutrient requirements of suspension cultures of soybean root cells. *Exp Cell Res* **50**(1): 151-158.
- Gao C, Cai Y, Wang Y, Kang BH, Aniento F, Robinson DG, Jiang L. 2014.** Retention mechanisms for ER and Golgi membrane proteins. *Trends Plant Sci* **19**(8): 508-515.
- Garjeanne AJM. 1903.** Die Ölkörper der Jungermanniales. *Flora* **92**: 457-482.
- Geldner N, Denervaud-Tendon V, Hyman DL, Mayer U, Stierhof YD, Chory J. 2009.** Rapid, combinatorial analysis of membrane compartments in intact plants with a multicolor marker set. *Plant J* **59**(1): 169-178.
- Geldner N, Friml J, Stierhof YD, Jurgens G, Palme K. 2001.** Auxin transport inhibitors block PIN1 cycling and vesicle trafficking. *Nature* **413**(6854): 425-428.
- Grefen C, Chen Z, Honsbein A, Donald N, Hills A, Blatt MR. 2010.** A novel motif essential for SNARE interaction with the K⁺ channel KC1 and channel gating in *Arabidopsis*. *Plant Cell* **22**(9): 3076-3092.
- Grefen C, Karnik R, Larson E, Lefoulon C, Wang YZ, Waghmare S, Zhang B, Hills**

- A, Blatt MR. 2015.** A vesicle-trafficking protein commandeers Kv channel voltage sensors for voltage-dependent secretion. *Nature Plants* **1**(10).
- Guindon S, Dufayard JF, Lefort V, Anisimova M, Hordijk W, Gascuel O. 2010.** New algorithms and methods to estimate maximum-likelihood phylogenies: assessing the performance of PhyML 3.0. *Syst Biol* **59**(3): 307-321.
- Gutierrez R, Lindeboom JJ, Paredes AR, Emons AM, Ehrhardt DW. 2009.** Arabidopsis cortical microtubules position cellulose synthase delivery to the plasma membrane and interact with cellulose synthase trafficking compartments. *Nat Cell Biol* **11**(7): 797-806.
- Haga N, Kato K, Murase M, Araki S, Kubo M, Demura T, Suzuki K, Muller I, Voss U, Jurgens G, Ito M. 2007.** R1R2R3-Myb proteins positively regulate cytokinesis through activation of KNOLLE transcription in *Arabidopsis thaliana*. *Development* **134**(6): 1101-1110.
- Haga N, Kobayashi K, Suzuki T, Maeo K, Kubo M, Ohtani M, Mitsuda N, Demura T, Nakamura K, Jurgens G, Ito M. 2011.** Mutations in MYB3R1 and MYB3R4 cause pleiotropic developmental defects and preferential down-regulation of multiple G2/M-specific genes in Arabidopsis. *Plant Physiol* **157**(2): 706-717.
- Hardwick KG, Pelham HR. 1992.** SED5 encodes a 39-kD integral membrane protein required for vesicular transport between the ER and the Golgi complex. *J Cell Biol* **119**(3): 513-521.
- Hashiguchi Y, Yano D, Nagafusa K, Kato T, Saito C, Uemura T, Ueda T, Nakano A, Tasaka M, Terao Morita M. 2014.** A unique HEAT repeat-containing protein SHOOT GRAVITROPISM6 is involved in vacuolar membrane dynamics in gravity-sensing cells of Arabidopsis inflorescence stem. *Plant Cell Physiol* **55**(4): 811-822.
- He-Nyngren XA, I.; Julen, A.; Glenny, D.; Piippo, S. 2004.** Phylogeny of liverworts - beyond a leaf and a thallus. *Monogr. Syst. Bot. Mo. Bot. Gard.* **98**: 87 - 118.
- He-Nyngren XJ, A.; Ahonen, I.; Glenny, D.; Piippo, S. 2006.** Illuminating evolutionary history of liverworts (Marchantiophyta) - towards a natural classification. *Cladistics* **22**: 1 -31.
- He X, Sun Y, Zhu R-L. 2013.** The oil bodies of liverworts: Unique and important organelles in land plants. *Crit Rev Plant Sci* **32**(5): 293-302.
- Heese M, Gansel X, Sticher L, Wick P, Grebe M, Granier F, Jürgens G. 2001.** Functional characterization of the KNOLLE-interacting t-SNARE AtSNAP33 and its role in plant cytokinesis. *J Cell Biol* **155**(2): 239-249.
- Hong W. 2005.** SNAREs and traffic. *Biochim Biophys Acta* **1744**(2): 120-144.

- Honsbein A, Sokolovski S, Grefen C, Campanoni P, Pratelli R, Paneque M, Chen Z, Johansson I, Blatt MR. 2009.** A tripartite SNARE-K⁺ channel complex mediates in channel-dependent K⁺ nutrition in Arabidopsis. *Plant Cell* **21**(9): 2859-2877.
- Hori K, Maruyama F, Fujisawa T, Togashi T, Yamamoto N, Seo M, Sato S, Yamada T, Mori H, Tajima N, Moriyama T, Ikeuchi M, Watanabe M, Wada H, Kobayashi K, Saito M, Masuda T, Sasaki-Sekimoto Y, Mashiguchi K, Awai K, Shimojima M, Masuda S, Iwai M, Nobusawa T, Narise T, Kondo S, Saito H, Sato R, Murakawa M, Ihara Y, Oshima-Yamada Y, Ohtaka K, Satoh M, Sonobe K, Ishii M, Ohtani R, Kanamori-Sato M, Honoki R, Miyazaki D, Mochizuki H, Umetsu J, Higashi K, Shibata D, Kamiya Y, Sato N, Nakamura Y, Tabata S, Ida S, Kurokawa K, Ohta H. 2014.** *Klebsormidium flaccidum* genome reveals primary factors for plant terrestrial adaptation. *Nat Commun* **5**: 3978.
- Horn PJ, Ledbetter NR, James CN, Hoffman WD, Case CR, Verbeck GF, Chapman KD. 2011.** Visualization of lipid droplet composition by direct organelle mass spectrometry. *J Biol Chem* **286**(5): 3298-3306.
- Huang AHC. 1992.** Oil bodies and oleosins in seeds. *Annu Rev Plant Physiol Plant Mol Biol* **43**: 177-200.
- Huang CY, Chung CI, Lin YC, Hsing YI, Huang AH. 2009.** Oil bodies and oleosins in *Physcomitrella* possess characteristics representative of early trends in evolution. *Plant Physiol* **150**(3): 1192-1203.
- Huang NL, Huang MD, Chen TL, Huang AH. 2013.** Oleosin of subcellular lipid droplets evolved in green algae. *Plant Physiol* **161**(4): 1862-1874.
- Huang WJ, Wu CL, Lin CW, Chi LL, Chen PY, Chiu CJ, Huang CY, Chen CN. 2010.** Marchantin A, a cyclic bis(bibenzyl ether), isolated from the liverwort *Marchantia emarginata* subsp. *tosana* induces apoptosis in human MCF-7 breast cancer cells. *Cancer Lett* **291**(1): 108-119.
- Ichikawa M, Hirano T, Enami K, Fuselier T, Kato N, Kwon C, Voigt B, Schulze-Lefert P, Baluska F, Sato MH. 2014.** Syntaxin of plant proteins SYP123 and SYP132 mediate root hair tip growth in *Arabidopsis thaliana*. *Plant Cell Physiol* **55**(4): 790-800.
- Inada N, Ueda T. 2014.** Membrane trafficking pathways and their roles in plant-microbe interactions. *Plant Cell Physiol* **55**(4): 672-686.
- International Rice Genome Sequencing P. 2005.** The map-based sequence of the rice genome. *Nature* **436**(7052): 793-800.
- Ishizaki K, Chiyoda S, Yamato KT, Kohchi T. 2008.** Agrobacterium-mediated

- transformation of the haploid liverwort *Marchantia polymorpha* L., an emerging model for plant biology. *Plant Cell Physiol* **49**(7): 1084-1091.
- Ishizaki K, Johzuka-Hisatomi Y, Ishida S, Iida S, Kohchi T. 2013.** Homologous recombination-mediated gene targeting in the liverwort *Marchantia polymorpha* L. *Sci Rep* **3**: 1532.
- Ishizaki K, Nishihama R, Ueda M, Inoue K, Ishida S, Nishimura Y, Shikanai T, Kohchi T. 2015.** Development of gateway binary vector series with four different selection markers for the liverwort *Marchantia polymorpha*. *PLoS One* **10**(9): e0138876.
- Itakura E, Kishi-Itakura C, Mizushima N. 2012.** The hairpin-type tail-anchored SNARE syntaxin 17 targets to autophagosomes for fusion with endosomes/lysosomes. *Cell* **151**(6): 1256-1269.
- Ito E, Fujimoto M, Ebine K, Uemura T, Ueda T, Nakano A. 2012.** Dynamic behavior of clathrin in *Arabidopsis thaliana* unveiled by live imaging. *Plant J* **69**(2): 204-216.
- Ito M, Araki S, Matsunaga S, Itoh T, Nishihama R, Machida Y, Doonan JH, Watanabe A. 2001.** G2/M-phase-specific transcription during the plant cell cycle is mediated by c-Myb-like transcription factors. *Plant Cell* **13**(8): 1891-1905.
- Ito Y, Uemura T, Nakano A. 2014.** Formation and maintenance of the Golgi apparatus in plant cells. *Int Rev Cell Mol Biol* **310**: 221-287.
- Ito Y, Uemura T, Shoda K, Fujimoto M, Ueda T, Nakano A. 2012.** *cis*-Golgi proteins accumulate near the ER exit sites and act as the scaffold for Golgi regeneration after brefeldin A treatment in tobacco BY-2 cells. *Mol Biol Cell* **23**(16): 3203-3214.
- Iwai Y, Murakami K, Gomi Y, Hashimoto T, Asakawa Y, Okuno Y, Ishikawa T, Hatakeyama D, Echigo N, Kuzuhara T. 2011.** Anti-influenza activity of marchantins, macrocyclic bisbibenzyls contained in liverworts. *PLoS One* **6**(5): e19825.
- Jürgens G, Park M, Richter S, Touihri S, Krause C, El Kasmi F, Mayer U. 2015.** Plant cytokinesis: a tale of membrane traffic and fusion. *Biochem Soc Trans* **43**(1): 73-78.
- Jia Q, Li G, Kollner TG, Fu J, Chen X, Xiong W, Crandall-Stotler BJ, Bowman JL, Weston DJ, Zhang Y, Chen L, Xie Y, Li FW, Rothfels CJ, Larsson A, Graham SW, Stevenson DW, Wong GK, Gershenzon J, Chen F. 2016.** Microbial-type terpene synthase genes occur widely in nonseed land plants, but not in seed plants. *Proc Natl Acad Sci U S A* **113**(43): 12328-12333.

- Jones DT, Taylor WR, Thornton JM. 1992.** The rapid generation of mutation data matrices from protein sequences. *Comput Appl Biosci* **8**(3): 275-282.
- Küster W. 1894.** Die Oelkörper der Lebermoose und ihr Verhältniss zu den Elaioplasten. *Basel*.
- Kamory E, Keseru GM, Papp B. 1995.** Isolation and antibacterial activity of marchantin A, a cyclic bis(bibenzyl) constituent of Hungarian *Marchantia polymorpha*. *Planta Med* **61**(4): 387-388.
- Kanazawa T, Era A, Minamino N, Shikano Y, Fujimoto M, Uemura T, Nishihama R, Yamato KT, Ishizaki K, Nishiyama T, Kohchi T, Nakano A, Ueda T. 2016.** SNARE molecules in *Marchantia polymorpha*: Unique and conserved features of the membrane fusion machinery. *Plant Cell Physiol* **57**(2): 307-324.
- Kanazawa T, Ishizaki K, Kohchi T, Hanaoka M, Tanaka K. 2013.** Characterization of four nuclear-encoded plastid RNA polymerase sigma factor genes in the liverwort *Marchantia polymorpha*: blue-light- and multiple stress-responsive SIG5 was acquired early in the emergence of terrestrial plants. *Plant Cell Physiol* **54**(10): 1736-1748.
- Kanazawa T, Era A, Ueda, T. 2015.** Spectral imaging: a powerful tool for confocal multicolor imaging in living plant cells. *Zeiss Application Note*.
- Karimi M, De Meyer B, Hilson P. 2005.** Modular cloning in plant cells. *Trends Plant Sci* **10**(3): 103-105.
- Kato H, Ishizaki K, Kouno M, Shirakawa M, Bowman JL, Nishihama R, Kohchi T. 2015.** Auxin-mediated transcriptional system with a minimal set of components is critical for morphogenesis through the life cycle in *Marchantia polymorpha*. *PLoS Genet* **11**(5): e1005084.
- Kato T, Morita MT, Fukaki H, Yamauchi Y, Uehara M, Niihama M, Tasaka M. 2002.** SGR2, a phospholipase-like protein, and ZIG/SGR4, a SNARE, are involved in the shoot gravitropism of Arabidopsis. *Plant Cell* **14**(1): 33-46.
- Katoh K, Toh H. 2008.** Recent developments in the MAFFT multiple sequence alignment program. *Brief Bioinform* **9**(4): 286-298.
- Katsaros CI, Varvarigos V, Gachon CM, Brand J, Motomura T, Nagasato C, Kupper FC. 2011.** Comparative immunofluorescence and ultrastructural analysis of microtubule organization in *Uronema* sp., *Klebsormidium flaccidum*, *K. subtilissimum*, *Stichococcus bacillaris* and *S. chloranthus* (Chlorophyta). *Protist* **162**(2): 315-331.
- Kim SJ, Brandizzi F. 2014.** The plant secretory pathway: an essential factory for building the plant cell wall. *Plant Cell Physiol* **55**(4): 687-693.

- Kirchhelle C, Chow CM, Foucart C, Neto H, Stierhof YD, Kalde M, Walton C, Fricker M, Smith RS, Jerusalem A, Irani N, Moore I. 2016.** The specification of geometric edges by a plant Rab GTPase is an essential cell-patterning principle during organogenesis in Arabidopsis. *Dev Cell* **36**(4): 386-400.
- Kloepper TH, Kienle CN, Fasshauer D. 2007.** An elaborate classification of SNARE proteins sheds light on the conservation of the eukaryotic endomembrane system. *Mol Biol Cell* **18**(9): 3463-3471.
- Klopper TH, Kienle N, Fasshauer D, Munro S. 2012.** Untangling the evolution of Rab G proteins: implications of a comprehensive genomic analysis. *BMC Biol* **10**: 71.
- Kohchi T, Ishizaki, K. 2012.** Liverwort, *Marchantia polymorpha* L., as a reviving model for plant biology. *BSJ Review* **3**: 58-70.
- Kozlowski A. 1921.** Sur l'origine des oleoleucites chez les hépatiques à feuilles. *C. R. Acad. Sci. Paris* **173**: 497-499.
- Kubota A, Ishizaki K, Hosaka M, Kohchi T. 2013.** Efficient Agrobacterium-mediated transformation of the liverwort *Marchantia polymorpha* using regenerating thalli. *Biosci Biotechnol Biochem* **77**(1): 167-172.
- Kumar S, Kempinski C, Zhuang X, Norris A, Mafu S, Zi J, Bell SA, Nybo SE, Kinison SE, Jiang Z, Goklany S, Linscott KB, Chen X, Jia Q, Brown SD, Bowman JL, Babbitt PC, Peters RJ, Chen F, Chappell J. 2016.** Molecular diversity of terpene synthases in the liverwort *Marchantia polymorpha*. *Plant Cell* **28**(10): 2632-2650.
- Kwon C, Neu C, Pajonk S, Yun HS, Lipka U, Humphry M, Bau S, Straus M, Kwaaitaal M, Rampelt H, El Kasmi F, Jurgens G, Parker J, Panstruga R, Lipka V, Schulze-Lefert P. 2008.** Co-option of a default secretory pathway for plant immune responses. *Nature* **451**(7180): 835-840.
- Lauber MH, Waizenegger I, Steinmann T, Schwarz H, Mayer U, Hwang I, Lukowitz W, Jurgens G. 1997.** The Arabidopsis KNOLLE protein is a cytokinesis-specific syntaxin. *J Cell Biol* **139**(6): 1485-1493.
- Le SQ, Lartillot N, Gascuel O. 2008.** Phylogenetic mixture models for proteins. *Philos Trans R Soc Lond B Biol Sci* **363**(1512):3965-3976.
- Leshem Y, Melamed-Book N, Cagnac O, Ronen G, Nishri Y, Solomon M, Cohen G, Levine A. 2006.** Suppression of Arabidopsis vesicle-SNARE expression inhibited fusion of H₂O₂-containing vesicles with tonoplast and increased salt tolerance. *Proc Natl Acad Sci U S A* **103**(47): 18008-18013.
- Lewis MJ, Pelham HR. 1996.** SNARE-mediated retrograde traffic from the Golgi complex to the endoplasmic reticulum. *Cell* **85**(2): 205-215.

- Lewis MJ, Rayner JC, Pelham HR. 1997.** A novel SNARE complex implicated in vesicle fusion with the endoplasmic reticulum. *EMBO J* **16**(11): 3017-3024.
- Liu YG, Mitsukawa N, Oosumi T, Whittier RF. 1995.** Efficient isolation and mapping of *Arabidopsis thaliana* T-DNA insert junctions by thermal asymmetric interlaced PCR. *Plant J* **8**(3): 457-463.
- Lukowitz W, Mayer U, Jürgens G. 1996.** Cytokinesis in the Arabidopsis embryo involves the syntaxin-related KNOLLE gene product. *Cell* **84**(1): 61-71.
- Müller I, Wagner W, Völker A, Schellmann S, Nacry P, Kuttner F, Schwarz-Sommer Z, Mayer U, Jürgens G. 2003.** Syntaxin specificity of cytokinesis in Arabidopsis. *Nat Cell Biol* **5**(6): 531-534.
- Müller K. 1939.** Untersuchungen über die Ölkörper der Lebermoose. *Berichte der Deutschen Botanischen Gesellschaft* **57**: 326 - 370.
- Müller S, Jürgens G. 2016.** Plant cytokinesis-No ring, no constriction but centrifugal construction of the partitioning membrane. *Semin Cell Dev Biol* **53**: 10-18.
- Maddison D, Maddison W. 2000.** MacClade 4: Analysis of phylogeny and character evolution. Sunderland, MA: Sinauer Associates, Inc., Publishers.
- Marchant HJ, Pickett-Heaps JD. 1973.** Mitosis and cytokinesis in *Coleochaete scutata*. *J Phycol* **9**(4): 461-471.
- Marti L, Fornaciari S, Renna L, Stefano G, Brandizzi F. 2010.** COPII-mediated traffic in plants. *Trends Plant Sci* **15**(9): 522-528.
- Matsuzaki M, Misumi O, Shin IT, Maruyama S, Takahara M, Miyagishima SY, Mori T, Nishida K, Yagisawa F, Nishida K, Yoshida Y, Nishimura Y, Nakao S, Kobayashi T, Momoyama Y, Higashiyama T, Minoda A, Sano M, Nomoto H, Oishi K, Hayashi H, Ohta F, Nishizaka S, Haga S, Miura S, Morishita T, Kabeya Y, Terasawa K, Suzuki Y, Ishii Y, Asakawa S, Takano H, Ohta N, Kuroiwa H, Tanaka K, Shimizu N, Sugano S, Sato N, Nozaki H, Ogasawara N, Kohara Y, Kuroiwa T. 2004.** Genome sequence of the ultrasmall unicellular red alga *Cyanidioschyzon merolae* 10D. *Nature* **428**(6983): 653-657.
- Mayer U, Ruiz RAT, Berleth T, Misera S, Jürgens G. 1991.** Mutations affecting body organization in the Arabidopsis embryo. *Nature* **353**(6343): 402-407.
- McIntosh K, Pickettheaps JD, Gunning BES. 1995.** Cytokinesis in *Spirogyra* - integration of cleavage and cell-plate formation. *Int J Plant Sci* **156**(1): 1-8.
- Merchant SS, Prochnik SE, Vallon O, Harris EH, Karpowicz SJ, Witman GB, Terry A, Salamov A, Fritz-Laylin LK, Marechal-Drouard L, Marshall WF, Qu LH, Nelson DR, Sanderfoot AA, Spalding MH, Kapitonov VV, Ren Q, Ferris P, Lindquist E, Shapiro H, Lucas SM, Grimwood J, Schmutz J, Cardol P,**

- Cerutti H, Chanfreau G, Chen CL, Cognat V, Croft MT, Dent R, Dutcher S, Fernandez E, Fukuzawa H, Gonzalez-Ballester D, Gonzalez-Halphen D, Hallmann A, Hanikenne M, Hippler M, Inwood W, Jabbari K, Kalanon M, Kuras R, Lefebvre PA, Lemaire SD, Lobanov AV, Lohr M, Manuell A, Meier I, Mets L, Mittag M, Mittelmeier T, Moroney JV, Moseley J, Napoli C, Nedelcu AM, Niyogi K, Novoselov SV, Paulsen IT, Pazour G, Purton S, Ral JP, Riano-Pachon DM, Riekhof W, Rymarquis L, Schroda M, Stern D, Umen J, Willows R, Wilson N, Zimmer SL, Allmer J, Balk J, Bisova K, Chen CJ, Elias M, Gendler K, Hauser C, Lamb MR, Ledford H, Long JC, Minagawa J, Page MD, Pan J, Pootakham W, Roje S, Rose A, Stahlberg E, Terauchi AM, Yang P, Ball S, Bowler C, Dieckmann CL, Gladyshev VN, Green P, Jorgensen R, Mayfield S, Mueller-Roeber B, Rajamani S, Sayre RT, Brokstein P, Dubchak I, Goodstein D, Hornick L, Huang YW, Jhaveri J, Luo Y, Martinez D, Ngau WC, Otilar B, Poliakov A, Porter A, Szajkowski L, Werner G, Zhou K, Grigoriev IV, Rokhsar DS, Grossman AR. 2007. The *Chlamydomonas* genome reveals the evolution of key animal and plant functions. *Science* 318(5848): 245-250.
- Mirbel C-F. 1835. Recherches anatomique et physiologique sur le *Marchantia polymorpha*. *Mém. Acad. Roy. Sc. Inst. France* 13: 337-436.
- Morita MT, Kato T, Nagafusa K, Saito C, Ueda T, Nakano A, Tasaka M. 2002. Involvement of the vacuoles of the endodermis in the early process of shoot gravitropism in Arabidopsis. *Plant Cell* 14(1): 47-56.
- Muppirala M, Gupta V, Swarup G. 2011. Syntaxin 17 cycles between the ER and ERGIC and is required to maintain the architecture of ERGIC and Golgi. *Biol Cell* 103(7): 333-350.
- Napier JA, Stobart AK, Shewry PR. 1996. The structure and biogenesis of plant oil bodies: The role of the ER membrane and the oleosin class of proteins. *Plant Mol Biol* 31(5): 945-956.
- Neale DB, Wegrzyn JL, Stevens KA, Zimin AV, Puiu D, Crepeau MW, Cardeno C, Koriabine M, Holtz-Morris AE, Liechty JD, Martinez-Garcia PJ, Vasquez-Gross HA, Lin BY, Zieve JJ, Dougherty WM, Fuentes-Soriano S, Wu LS, Gilbert D, Marcais G, Roberts M, Holt C, Yandell M, Davis JM, Smith KE, Dean JF, Lorenz WW, Whetten RW, Sederoff R, Wheeler N, McGuire PE, Main D, Loopstra CA, Mockaitis K, deJong PJ, Yorke JA, Salzberg SL, Langley CH. 2014. Decoding the massive genome of loblolly pine using haploid DNA and novel assembly strategies. *Genome Biol* 15(3): R59.

- Newman AP, Shim J, Ferro-Novick S. 1990.** BET1, BOS1, and SEC22 are members of a group of interacting yeast genes required for transport from the endoplasmic reticulum to the Golgi complex. *Mol Cell Biol* **10**(7): 3405-3414.
- Nichols BJ, Pelham HR. 1998.** SNAREs and membrane fusion in the Golgi apparatus. *Biochim Biophys Acta* **1404**(1-2): 9-31.
- Nielsen ME, Feechan A, Bohlenius H, Ueda T, Thordal-Christensen H. 2012.** Arabidopsis ARF-GTP exchange factor, GNOM, mediates transport required for innate immunity and focal accumulation of syntaxin PEN1. *Proc Natl Acad Sci U S A* **109**(28): 11443-11448.
- Nielsen ME, Thordal-Christensen H. 2012.** Recycling of Arabidopsis plasma membrane PEN1 syntaxin. *Plant Signal Behav* **7**(12): 1541-1543.
- Niihama M, Uemura T, Saito C, Nakano A, Sato MH, Tasaka M, Morita MT. 2005.** Conversion of functional specificity in Qb-SNARE VTI1 homologues of Arabidopsis. *Curr Biol* **15**(6): 555-560.
- Niu C, Qu JB, Lou HX. 2006.** Antifungal bis[bibenzyls] from the Chinese liverwort *Marchantia polymorpha* L. *Chem Biodivers* **3**(1): 34-40.
- Nozaki H, Takano H, Misumi O, Terasawa K, Matsuzaki M, Maruyama S, Nishida K, Yagisawa F, Yoshida Y, Fujiwara T, Takio S, Tamura K, Chung SJ, Nakamura S, Kuroiwa H, Tanaka K, Sato N, Kuroiwa T. 2007.** A 100%-complete sequence reveals unusually simple genomic features in the hot-spring red alga *Cyanidioschyzon merolae*. *BMC Biol* **5**: 28.
- Ohtomo I, Ueda H, Shimada T, Nishiyama C, Komoto Y, Hara-Nishimura I, Takahashi T. 2005.** Identification of an allele of VAM3/SYP22 that confers a semi-dwarf phenotype in *Arabidopsis thaliana*. *Plant Cell Physiol* **46**(8): 1358-1365.
- Otegui MS, Mastrorarde DN, Kang BH, Bednarek SY, Staehelin LA. 2001.** Three-dimensional analysis of syncytial-type cell plates during endosperm cellularization visualized by high resolution electron tomography. *Plant Cell* **13**(9): 2033-2051.
- Palenik B, Grimwood J, Aerts A, Rouze P, Salamov A, Putnam N, Dupont C, Jorgensen R, Derelle E, Rombauts S, Zhou K, Otiillar R, Merchant SS, Podell S, Gaasterland T, Napoli C, Gendler K, Manuell A, Tai V, Vallon O, Piganeau G, Jancek S, Heijde M, Jabbari K, Bowler C, Lohr M, Robbens S, Werner G, Dubchak I, Pazour GJ, Ren Q, Paulsen I, Delwiche C, Schmutz J, Rokhsar D, Van de Peer Y, Moreau H, Grigoriev IV. 2007.** The tiny eukaryote *Ostreococcus* provides genomic insights into the paradox of plankton speciation.

- Proc Natl Acad Sci U S A* **104**(18): 7705-7710.
- Park E, Diaz-Moreno SM, Davis DJ, Wilkop TE, Bulone V, Drakakaki G. 2014.** Endosidin 7 specifically arrests late cytokinesis and inhibits callose biosynthesis, revealing distinct trafficking events during cell plate maturation. *Plant Physiol* **165**(3): 1019-1034.
- Pearse BM. 1975.** Coated vesicles from pig brain: purification and biochemical characterization. *J Mol Biol* **97**(1): 93-98.
- Petrasek J, Mravec J, Bouchard R, Blakeslee JJ, Abas M, Seifertova D, Wisniewska J, Tadele Z, Kubes M, Covanova M, Dhonukshe P, Skupa P, Benkova E, Perry L, Krecek P, Lee OR, Fink GR, Geisler M, Murphy AS, Luschnig C, Zazimalova E, Friml J. 2006.** PIN proteins perform a rate-limiting function in cellular auxin efflux. *Science* **312**(5775): 914-918.
- Pfeffer W. 1874.** Die Oelkörper der Lebermoose. *Flora* **57**: 2-6, 17-27, 33-43.
- Pickett-Heaps JD. 1967.** Ultrastructure and Differentiation in *Chara* sp. II. Mitosis. *Aust J Biol Sci* **20**(5): 883-894.
- Pickett-Heaps JD. 1972.** Cell division in *Klebsormidium subtilissimum* (formerly *Ulothrix subtilissima*) and its possible phylogenetic significance. *Cytobios* **6**: 167-183.
- Pressel S, Duckett JG, Ligrone R, Proctor MCF. 2009.** Effects of de- and rehydration in desiccation-tolerant liverworts: A cytological and physiological study. *Int J Plant Sci* **170**(2): 182-199.
- Proust H, Honkanen S, Jones VA, Morieri G, Prescott H, Kelly S, Ishizaki K, Kohchi T, Dolan L. 2016.** RSL Class I genes controlled the development of epidermal structures in the common ancestor of land plants. *Curr Biol* **26**(1): 93-99.
- Qiu YL, Li L, Wang B, Chen Z, Knoop V, Groth-Malonek M, Dombrovskaya O, Lee J, Kent L, Rest J, Estabrook GF, Hendry TA, Taylor DW, Testa CM, Ambros M, Crandall-Stotler B, Duff RJ, Stech M, Frey W, Quandt D, Davis CC. 2006.** The deepest divergences in land plants inferred from phylogenomic evidence. *Proc Natl Acad Sci U S A* **103**(42): 15511-15516.
- Reichardt I, Slane D, El Kasmi F, Knoll C, Fuchs R, Mayer U, Lipka V, Jürgens G. 2011.** Mechanisms of functional specificity among plasma-membrane syntaxins in Arabidopsis. *Traffic* **12**(9): 1269-1280.
- Reichardt I, Stierhof YD, Mayer U, Richter S, Schwarz H, Schumacher K, Jürgens G. 2007.** Plant cytokinesis requires de novo secretory trafficking but not endocytosis. *Curr Biol* **17**(23): 2047-2053.
- Rensing SA, Ick J, Fawcett JA, Lang D, Zimmer A, Van de Peer Y, Reski R. 2007.**

An ancient genome duplication contributed to the abundance of metabolic genes in the moss *Physcomitrella patens*. *BMC Evol Biol* 7: 130.

- Rensing SA, Lang D, Zimmer AD, Terry A, Salamov A, Shapiro H, Nishiyama T, Perroud PF, Lindquist EA, Kamisugi Y, Tanahashi T, Sakakibara K, Fujita T, Oishi K, Shin IT, Kuroki Y, Toyoda A, Suzuki Y, Hashimoto S, Yamaguchi K, Sugano S, Kohara Y, Fujiyama A, Anterola A, Aoki S, Ashton N, Barbazuk WB, Barker E, Bennetzen JL, Blankenship R, Cho SH, Dutcher SK, Estelle M, Fawcett JA, Gundlach H, Hanada K, Heyl A, Hicks KA, Hughes J, Lohr M, Mayer K, Melkozernov A, Murata T, Nelson DR, Pils B, Prigge M, Reiss B, Renner T, Rombauts S, Rushton PJ, Sanderfoot A, Schween G, Shiu SH, Stueber K, Theodoulou FL, Tu H, Van de Peer Y, Verrier PJ, Waters E, Wood A, Yang L, Cove D, Cuming AC, Hasebe M, Lucas S, Mishler BD, Reski R, Grigoriev IV, Quatrano RS, Boore JL. 2008.** The *Physcomitrella* genome reveals evolutionary insights into the conquest of land by plants. *Science* 319(5859): 64-69.
- Richter S, Geldner N, Schrader J, Wolters H, Stierhof YD, Rios G, Koncz C, Robinson DG, Jürgens G. 2007.** Functional diversification of closely related ARF-GEFs in protein secretion and recycling. *Nature* 448(7152): 488-492.
- Richter S, Kientz M, Brumm S, Nielsen ME, Park M, Gavidia R, Krause C, Voss U, Beckmann H, Mayer U, Stierhof YD, Jürgens G. 2014.** Delivery of endocytosed proteins to the cell-division plane requires change of pathway from recycling to secretion. *Elife* 3: e02131.
- Richter S, Voss U, Jürgens G. 2009.** Post-Golgi traffic in plants. *Traffic* 10(7): 819-828.
- Robert S, Chary SN, Drakakaki G, Li S, Yang Z, Raikhel NV, Hicks GR. 2008.** Endosidin1 defines a compartment involved in endocytosis of the brassinosteroid receptor BRI1 and the auxin transporters PIN2 and AUX1. *Proc Natl Acad Sci U S A* 105(24): 8464-8469.
- Robinson DG, Jiang L, Schumacher K. 2008.** The endosomal system of plants: charting new and familiar territories. *Plant Physiol* 147(4): 1482-1492.
- Rutherford S, Moore I. 2002.** The Arabidopsis Rab GTPase family: another enigma variation. *Curr Opin Plant Biol* 5(6): 518-528.
- Rybak K, Steiner A, Synek L, Klaeger S, Kulich I, Facher E, Wanner G, Kuster B, Zarsky V, Persson S, Assaad FF. 2014.** Plant cytokinesis is orchestrated by the sequential action of the TRAPP II and exocyst tethering complexes. *Dev Cell* 29(5): 607-620.
- Saito C, Ueda T. 2009.** Chapter 4: Functions of RAB and SNARE proteins in plant life.

- Int Rev Cell Mol Biol* **274**: 183-233.
- Saito C, Ueda T, Abe H, Wada Y, Kuroiwa T, Hisada A, Furuya M, Nakano A. 2002.** A complex and mobile structure forms a distinct subregion within the continuous vacuolar membrane in young cotyledons of *Arabidopsis*. *Plant J* **29**(3): 245-255.
- Saitou N, Nei M. 1987.** The neighbor-joining method: a new method for reconstructing phylogenetic trees. *Mol Biol Evol* **4**(4): 406-425.
- Samuels AL, Giddings TH, Jr., Staehelin LA. 1995.** Cytokinesis in tobacco BY-2 and root tip cells: a new model of cell plate formation in higher plants. *J Cell Biol* **130**(6): 1345-1357.
- Sanderfoot A. 2007.** Increases in the number of SNARE genes parallels the rise of multicellularity among the green plants. *Plant Physiol* **144**(1): 6-17.
- Sanderfoot AA, Assaad FF, Raikhel NV. 2000.** The *Arabidopsis* genome. An abundance of soluble *N*-ethylmaleimide-sensitive factor adaptor protein receptors. *Plant Physiol* **124**(4): 1558-1569.
- Sanderfoot AA, Kovaleva V, Bassham DC, Raikhel NV. 2001a.** Interactions between syntaxins identify at least five SNARE complexes within the Golgi/prevacuolar system of the *Arabidopsis* cell. *Mol Biol Cell* **12**(12): 3733-3743.
- Sanderfoot AA, Kovaleva V, Zheng H, Raikhel NV. 1999.** The t-SNARE AtVAM3p resides on the prevacuolar compartment in *Arabidopsis* root cells. *Plant Physiol* **121**(3): 929-938.
- Sanderfoot AA, Pilgrim M, Adam L, Raikhel NV. 2001b.** Disruption of individual members of *Arabidopsis* syntaxin gene families indicates each has essential functions. *Plant Cell* **13**(3): 659-666.
- Sanmartin M, Ordonez A, Sohn EJ, Robert S, Sanchez-Serrano JJ, Surpin MA, Raikhel NV, Rojo E. 2007.** Divergent functions of VTI12 and VTI11 in trafficking to storage and lytic vacuoles in *Arabidopsis*. *Proc Natl Acad Sci U S A* **104**(9): 3645-3650.
- Sato MH, Nakamura N, Ohsumi Y, Kouchi H, Kondo M, Hara-Nishimura I, Nishimura M, Wada Y. 1997.** The AtVAM3 encodes a syntaxin-related molecule implicated in the vacuolar assembly in *Arabidopsis thaliana*. *J Biol Chem* **272**(39): 24530-24535.
- Scheuring D, Viotti C, Kruger F, Kunzl F, Sturm S, Bubeck J, Hillmer S, Frigerio L, Robinson DG, Pimpl P, Schumacher K. 2011.** Multivesicular bodies mature from the *trans*-Golgi network/early endosome in *Arabidopsis*. *Plant Cell* **23**(9): 3463-3481.
- Schuster RM. 1966.** The Hepaticae and Anthocerotae of North America, Vol. I. *Columbia*

University Press, New York.

- Segami S, Makino S, Miyake A, Asaoka M, Maeshima M. 2014.** Dynamics of vacuoles and H⁺-pyrophosphatase visualized by monomeric green fluorescent protein in *Arabidopsis*: artifactual bulbs and native intravacuolar spherical structures. *Plant Cell* **26**(8): 3416-3434.
- Segui-Simarro JM, Austin JR, 2nd, White EA, Staehelin LA. 2004.** Electron tomographic analysis of somatic cell plate formation in meristematic cells of *Arabidopsis* preserved by high-pressure freezing. *Plant Cell* **16**(4): 836-856.
- Shimada TL, Shimada T, Hara-Nishimura I. 2010.** A rapid and non-destructive screenable marker, FAST, for identifying transformed seeds of *Arabidopsis thaliana*. *Plant J* **61**(3): 519-528.
- Shirakawa M, Ueda H, Shimada T, Koumoto Y, Shimada TL, Kondo M, Takahashi T, Okuyama Y, Nishimura M, Hara-Nishimura I. 2010.** Arabidopsis Qa-SNARE SYP2 proteins localized to different subcellular regions function redundantly in vacuolar protein sorting and plant development. *Plant J* **64**(6): 924-935.
- Singh MK, Kruger F, Beckmann H, Brumm S, Vermeer JE, Munnik T, Mayer U, Stierhof YD, Grefen C, Schumacher K, Jurgens G. 2014.** Protein delivery to vacuole requires SAND protein-dependent Rab GTPase conversion for MVB-vacuole fusion. *Curr Biol* **24**(12): 1383-1389.
- Sollner T, Bennett MK, Whiteheart SW, Scheller RH, Rothman JE. 1993a.** A protein assembly-disassembly pathway in vitro that may correspond to sequential steps of synaptic vesicle docking, activation, and fusion. *Cell* **75**(3): 409-418.
- Sollner T, Whiteheart SW, Brunner M, Erdjument-Bromage H, Geromanos S, Tempst P, Rothman JE. 1993b.** SNAP receptors implicated in vesicle targeting and fusion. *Nature* **362**(6418): 318-324.
- Stahl E. 1888.** Pflanzen und Schnecken. *Jena Z Med Naturwiss* **22**: 557 - 684.
- Stegmaier M, Oorschot V, Klumperman J, Scheller RH. 2000.** Syntaxin 17 is abundant in steroidogenic cells and implicated in smooth endoplasmic reticulum membrane dynamics. *Mol Biol Cell* **11**(8): 2719-2731.
- Sugano SS, Shirakawa M, Takagi J, Matsuda Y, Shimada T, Hara-Nishimura I, Kohchi T. 2014.** CRISPR/Cas9-mediated targeted mutagenesis in the liverwort *Marchantia polymorpha* L. *Plant Cell Physiol* **55**(3): 475-481.
- Suire C. 1970.** Recherches cytologiques sur deux Hépatiques: *Pellia epiphylla* (L.) Corda (Metzgeriale) and *Radula complanata* (L.) Dum. (Jungermanniale): ergastome, sporogénèse et spermatogénèse. *Botaniste* **53**: 125-392.

- Suire C. 2000.** A comparative, transmission-electron microscopic study on the formation of oil-bodies in liverworts. *J Hattori Bot Lab* **89**: 209-232.
- Suire C, Bouvier F, Backhaus RA, Begu D, Bonneau M, Camara B. 2000.** Cellular localization of isoprenoid biosynthetic enzymes in *Marchantia polymorpha*. Uncovering a new role of oil bodies. *Plant Physiol* **124**(3): 971-978.
- Sun S, Yu JP, Chen F, Zhao TJ, Fang XH, Li YQ, Sui SF. 2008.** TINY, a dehydration-responsive element (DRE)-binding protein-like transcription factor connecting the DRE- and ethylene-responsive element-mediated signaling pathways in Arabidopsis. *J Biol Chem* **283**(10): 6261-6271.
- Surpin M, Zheng H, Morita MT, Saito C, Avila E, Blakeslee JJ, Bandyopadhyay A, Kovaleva V, Carter D, Murphy A, Tasaka M, Raikhel N. 2003.** The VTI family of SNARE proteins is necessary for plant viability and mediates different protein transport pathways. *Plant Cell* **15**(12): 2885-2899.
- Sutter JU, Campanoni P, Tyrrell M, Blatt MR. 2006.** Selective mobility and sensitivity to SNAREs is exhibited by the Arabidopsis KAT1 K⁺ channel at the plasma membrane. *Plant Cell* **18**(4): 935-954.
- Suwastika IN, Uemura T, Shiina T, Sato MH, Takeyasu K. 2008.** SYP71, a plant-specific Qc-SNARE protein, reveals dual localization to the plasma membrane and the endoplasmic reticulum in Arabidopsis. *Cell Struct Funct* **33**(2): 185-192.
- Szponarski W, Sommerer N, Boyer JC, Rossignol M, Gibrat R. 2004.** Large-scale characterization of integral proteins from Arabidopsis vacuolar membrane by two-dimensional liquid chromatography. *Proteomics* **4**(2): 397-406.
- Tanaka H, Nodzyński T, Kitakura S, Feraru MI, Sasabe M, Ishikawa T, Kleine-Vehn J, Kakimoto T, Friml J. 2014.** BEX1/ARF1A1C is required for BFA-sensitive recycling of PIN Auxin transporters and Auxin-mediated development in Arabidopsis. *Plant Cell Physiol* **55**(4): 737-749.
- Tanaka M, Esaki T, Kenmoku H, Koeduka T, Kiyoyama Y, Masujima T, Asakawa Y, Matsui K. 2016.** Direct evidence of specific localization of sesquiterpenes and marchantin A in oil body cells of *Marchantia polymorpha* L. *Phytochemistry* **130**: 77-84.
- Tang H, Bowers JE, Wang X, Ming R, Alam M, Paterson AH. 2008.** Synteny and collinearity in plant genomes. *Science* **320**(5875): 486-488.
- Tsuboyama-Tanaka S, Kodama Y. 2015.** AgarTrap-mediated genetic transformation using intact gemmae/gemmalings of the liverwort *Marchantia polymorpha* L. *J Plant Res* **128**(2): 337-344.
- Tsuboyama S, Kodama Y. 2013.** AgarTrap: A simplified agrobacterium-mediated

transformation method for sporelings of the liverwort *Marchantia polymorpha* L. *Plant Cell Physiol* **55**(1): 229-236.

- Tuskan GA, Difazio S, Jansson S, Bohlmann J, Grigoriev I, Hellsten U, Putnam N, Ralph S, Rombauts S, Salamov A, Schein J, Sterck L, Aerts A, Bhalerao RR, Bhalerao RP, Blaudez D, Boerjan W, Brun A, Brunner A, Busov V, Campbell M, Carlson J, Chalot M, Chapman J, Chen GL, Cooper D, Coutinho PM, Couturier J, Covert S, Cronk Q, Cunningham R, Davis J, Degroeve S, Dejardin A, Depamphilis C, Detter J, Dirks B, Dubchak I, Duplessis S, Ehlting J, Ellis B, Gendler K, Goodstein D, Gribskov M, Grimwood J, Groover A, Gunter L, Hamberger B, Heinze B, Helariutta Y, Henrissat B, Holligan D, Holt R, Huang W, Islam-Faridi N, Jones S, Jones-Rhoades M, Jorgensen R, Joshi C, Kangasjarvi J, Karlsson J, Kelleher C, Kirkpatrick R, Kirst M, Kohler A, Kalluri U, Larimer F, Leebens-Mack J, Leple JC, Locascio P, Lou Y, Lucas S, Martin F, Montanini B, Napoli C, Nelson DR, Nelson C, Nieminen K, Nilsson O, Pereda V, Peter G, Philippe R, Pilate G, Poliakov A, Razumovskaya J, Richardson P, Rinaldi C, Ritland K, Rouze P, Ryaboy D, Schmutz J, Schrader J, Segerman B, Shin H, Siddiqui A, Sterky F, Terry A, Tsai CJ, Uberbacher E, Unneberg P, Vahala J, Wall K, Wessler S, Yang G, Yin T, Douglas C, Marra M, Sandberg G, Van de Peer Y, Rokhsar D. 2006.** The genome of black cottonwood, *Populus trichocarpa* (Torr. & Gray). *Science* **313**(5793): 1596-1604.
- Ueda T, Yamaguchi M, Uchimiya H, Nakano A. 2001.** Ara6, a plant-unique novel type Rab GTPase, functions in the endocytic pathway of *Arabidopsis thaliana*. *EMBO J* **20**(17): 4730-4741.
- Uehara M, Wang S, Kamiya T, Shigenobu S, Yamaguchi K, Fujiwara T, Naito S, Takano J. 2014.** Identification and characterization of an *Arabidopsis* mutant with altered localization of NIP5;1, a plasma membrane boric acid channel, reveals the requirement for D-galactose in endomembrane organization. *Plant Cell Physiol* **55**(4): 704-714.
- Uemura T. 2016.** Physiological roles of plant post-Golgi transport pathways in membrane trafficking. *Plant Cell Physiol* **57**(10): 2013-2019.
- Uemura T, Morita MT, Ebine K, Okatani Y, Yano D, Saito C, Ueda T, Nakano A. 2010.** Vacuolar/pre-vacuolar compartment Qa-SNAREs VAM3/SYP22 and PEP12/SYP21 have interchangeable functions in *Arabidopsis*. *Plant J* **64**(5): 864-873.
- Uemura T, Sato MH, Takeyasu K. 2005.** The longin domain regulates subcellular

- targeting of VAMP7 in *Arabidopsis thaliana*. *FEBS Lett* **579**(13): 2842-2846.
- Uemura T, Suda Y, Ueda T, Nakano A. 2014.** Dynamic behavior of the *trans*-Golgi network in root tissues of *Arabidopsis* revealed by super-resolution live imaging. *Plant Cell Physiol* **55**(4): 694-703.
- Uemura T, Ueda T. 2014.** Plant vacuolar trafficking driven by RAB and SNARE proteins. *Curr Opin Plant Biol* **22**: 116-121.
- Uemura T, Ueda T, Nakano A. 2012.** The physiological role of SYP4 in the salinity and osmotic stress tolerances. *Plant Signal Behav* **7**(9): 1118-1120.
- Uemura T, Ueda T, Ohniwa RL, Nakano A, Takeyasu K, Sato MH. 2004.** Systematic analysis of SNARE molecules in *Arabidopsis*: dissection of the post-Golgi network in plant cells. *Cell Struct Funct* **29**(2): 49-65.
- Völker A, Stierhof YD, Jürgens G. 2001.** Cell cycle-independent expression of the *Arabidopsis* cytokinesis-specific syntaxin KNOLLE results in mistargeting to the plasma membrane and is not sufficient for cytokinesis. *J Cell Sci* **114**(Pt 16): 3001-3012.
- Vance VB, Huang AHC. 1987.** The major protein from lipid bodies of maize - characterization and structure based on cDNA cloning. *J Biol Chem* **262**(23): 11275-11279.
- Viotti C, Bubeck J, Stierhof YD, Krebs M, Langhans M, van den Berg W, van Dongen W, Richter S, Geldner N, Takano J, Jurgens G, de Vries SC, Robinson DG, Schumacher K. 2010.** Endocytic and secretory traffic in *Arabidopsis* merge in the *trans*-Golgi network/early endosome, an independent and highly dynamic organelle. *Plant Cell* **22**(4): 1344-1357.
- Voeltz GK, Rolls MM, Rapoport TA. 2002.** Structural organization of the endoplasmic reticulum. *EMBO Rep* **3**(10): 944-950.
- Vukasinovic N, Zarsky V. 2016.** Tethering complexes in the *Arabidopsis* endomembrane system. *Front Cell Dev Biol* **4**: 46.
- Wakker JH. 1888.** Studien über die Inhaltkörper der Pflanzenzelle. *Jb wiss Bot* **19**: 482-487.
- Wei T, Zhang C, Hou X, Sanfacon H, Wang A. 2013.** The SNARE protein Syp71 is essential for turnip mosaic virus infection by mediating fusion of virus-induced vesicles with chloroplasts. *PLoS Pathog* **9**(5): e1003378.
- Wickett NJ, Mirarab S, Nguyen N, Warnow T, Carpenter E, Matasci N, Ayyampalayam S, Barker MS, Burleigh JG, Gitzendanner MA, Ruhfel BR, Wafula E, Der JP, Graham SW, Mathews S, Melkonian M, Soltis DE, Soltis PS, Miles NW, Rothfels CJ, Pokorny L, Shaw AJ, DeGironimo L, Stevenson**

- DW, Surek B, Villarreal JC, Roure B, Philippe H, dePamphilis CW, Chen T, Deyholos MK, Baucom RS, Kutchan TM, Augustin MM, Wang J, Zhang Y, Tian Z, Yan Z, Wu X, Sun X, Wong GK, Leebens-Mack J. 2014. Phylotranscriptomic analysis of the origin and early diversification of land plants. *Proc Natl Acad Sci U S A* **111**(45): E4859-4868.
- Wilson K, Long D, Swinburne J, Coupland G. 1996.** A Dissociation insertion causes a semidominant mutation that increases expression of TINY, an Arabidopsis gene related to APETALA2. *Plant Cell* **8**(4): 659-671.
- Wisniewska J, Xu J, Seifertova D, Brewer PB, Ruzicka K, Blilou I, Rouquie D, Benkova E, Scheres B, Friml J. 2006.** Polar PIN localization directs auxin flow in plants. *Science* **312**(5775): 883.
- Xue X, Sun DF, Sun CC, Liu HP, Yue B, Zhao CR, Lou HX, Qu XJ. 2012.** Inhibitory effect of riccardin D on growth of human non-small cell lung cancer: in vitro and in vivo studies. *Lung Cancer* **76**(3): 300-308.
- Yano D, Sato M, Saito C, Sato MH, Morita MT, Tasaka M. 2003.** A SNARE complex containing SGR3/AtVAM3 and ZIG/VTI11 in gravity-sensing cells is important for Arabidopsis shoot gravitropism. *Proc Natl Acad Sci U S A* **100**(14): 8589-8594.
- Yatsu LY, Jacks TJ. 1972.** Spherosome membranes - half unit-membranes. *Plant Physiol* **49**(6): 937-943.
- Zhang L, Zhang H, Liu P, Hao H, Jin JB, Lin J. 2011.** Arabidopsis R-SNARE proteins VAMP721 and VAMP722 are required for cell plate formation. *PLoS One* **6**(10): e26129.
- Zheng H, Bednarek SY, Sanderfoot AA, Alonso J, Ecker JR, Raikhel NV. 2002.** NPSN11 is a cell plate-associated SNARE protein that interacts with the syntaxin KNOLLE. *Plant Physiol* **129**(2): 530-539.
- Zheng H, von Mollard GF, Kovaleva V, Stevens TH, Raikhel NV. 1999.** The plant vesicle-associated SNARE AtVTI1a likely mediates vesicle transport from the *trans*-Golgi network to the prevacuolar compartment. *Mol Biol Cell* **10**(7): 2251-2264.
- Zimmer AD, Lang D, Buchta K, Rombauts S, Nishiyama T, Hasebe M, Van de Peer Y, Rensing SA, Reski R. 2013.** Reannotation and extended community resources for the genome of the non-seed plant *Physcomitrella patens* provide insights into the evolution of plant gene structures and functions. *BMC Genomics* **14**: 498.
- Zirkle C. 1932.** Vacuoles in primary meristems. *Z. Zellforsch* **16**: 26-47.
- Zouhar J, Rojo E, Bassham DC. 2009.** AtVPS45 is a positive regulator of the SYP41/SYP61/VTI12 SNARE complex involved in trafficking of vacuolar cargo.

Plant Physiol **149**(4): 1668-1678.